City Research Online

City, University of London Institutional Repository

This is the accepted version of the paper.

This version of the publication may differ from the final published version.

Income Uncertainty and the Decision to Invest in Bulk Shipping

Ioannis Kyriakou[*], Panos K. Pouliasis

Nikos C. Papapostolou and Nikos K. Nomikos

Cass Business School, City, University of London

106 Bunhill Row, London EC1Y 8TZ, UK

E-mails: ioannis.kyriakou@city.ac.uk; p_pouliasis@city.ac.uk;

n.papapostolou@city.ac.uk; n.nomikos@city.ac.uk

Abstract

We develop a coherent framework for the valuation of real assets and determination of the optimal time to invest. To this end, we model the stochastic nature of income and develop methodologies for valuing traded derivatives to facilitate model calibration and for assessing real investment projects. A valuation paradigm for freight-linked assets is presented and the effects of uncertainty in the key parameters are examined by means of a sensitivity analysis. Using a real option approach, we demonstrate its usefulness in investment appraisal and optimal timing of entry. We accompany our theoretical results with illustrative examples from the shipping industry.

Keywords: *real options, investment, uncertainty, contingent claims, shipping*

JEL classification: $C13$, $C63$, $G13$, $G31$, $L92$.

1 Introduction

Investment timing and uncertainty are issues that call for careful consideration when committing to any investment. Managers rely extensively on the use of traditional investment valuation criteria such as the Internal Rate of Return (IRR) and Net Present Value (NPV). These methods, although intuitive and easy to implement, have their shortcomings as the managerial flexibility implicit in any investment opportunity, i.e., the option to adapt investment decisions in response to uncertainty, is not taken into account, resulting in suboptimal investment timing rules. As such, managers often ignore or underestimate the extent of uncertainty and its implications. This can be dealt with by treating the investment decision as the exercise of an option under uncertainty, in which case real option theory provides better answers. In their seminal paper, Brennan and Schwartz (1985) evaluate natural resource investments based on arbitrage arguments, where uncertainty originates from the output price; operational policy decisions, such as postponing production temporarily or permanently, are also examined. Other early contributions on the use of real option theory in evaluating investment projects include McDonald and Siegel (1986), Majd and Pindyck (1987), Dixit (1989), Triantis and Hodder (1990) and Pindyck (1991); we refer to Dixit and Pindyck (1994) for a comprehensive literature survey. Typically, the payoff of the call option is a convex function of the underlying random variable, thus its value increases with uncertainty, i.e., the greater the uncertainty the greater the value of the option to invest and, hence, the incentive to keep the option open[1]; the investment decision is affected by the assessment of the option to either invest immediately or wait and observe the progress of the investment until market conditions improve. Hitherto, this is an issue that has been explored, inter alia, in different investment projects such as real estate (Grenadier, 1996), environmental technologies (Cortazar et al., 1998), natural resources (Schwartz and Smith, 2000, Moel and Tufano, 2002, Kellogg, 2014) and information technology (Schwartz and Zozaya-Gorostiza, 2003).

---

[1] An exception to this rule is identified in Kandel and Pearson (2002), who find that a negative relation may exist between the value of real options and uncertainty in the case of an incremental investment in technology aimed at reducing marginal costs of production.

This paper focuses on deep-sea shipping. This industry lends itself to this analysis as it is the backbone of international trade – 80% of global trade by volume and 70% of global trade by value are carried by sea and handled by ports (UNCTAD, 2015) – and a leading indicator of the global economy (Kilian, 2009) that has recently attracted much interest also in the finance and economics literature (e.g., see Kalouptsidi, 2014 and Papapostolou et al., 2014). Furthermore, the valuation of vessels has been traditionally based on the price that a well-informed rational investor would pay for the acquisition of a vessel using conventional investment criteria such as NPV. However, this static framework is unable to capture the market dynamics and the strategic optionalities available to shipping investors, such as the commitment of time and capital resources to order a vessel.

The key contribution of this paper is the development of a framework for evaluating real assets (ships in this case) and investing in based on a real-option based approach. The methodology is applied to the drybulk sector of the shipping industry which provides an ideal framework for empirical testing as there are numerous strategic and managerial flexibilities embedded in shipping investment and operation decisions (Alizadeh and Nomikos, 2009). Within this framework, two innovations are proposed. First, we derive a new, fast and accurate analytical method for pricing traded contingent claims on the discrete arithmetic average freight rate over a certain time interval[2] under spot freight rates represented by an exponential mean-reverting process with jumps of random magnitude and arrival. Using this, we then calibrate the model to real market data, verify it by performing relevant robustness checks, and, based on it, provide insights on how these assets can be evaluated; this is crucial as quite often research on real options is theoretical due to the lack of data for empirical testing. This also allows us to investigate the optimal timing of investment, the key drivers of the investment value, the price differences among vessels of different

---

[2]Options with an average based on finitely many asset values over time are called discrete average options as distinct from continuous average options. In practice, only discrete options are traded. Arithmetic average options are difficult to price as they do not have closed-form analytic solutions. The reason for this difficulty is that the payoff depends on the finite sum of correlated variables, for which there is no recognizable probability density function. In view of this limitation, we refer to Section 2.3 for more about how to deal with this option pricing problem.

economic lives and the impact of construction lags on the acquisition cost[3]. In fact, the importance of our formulation extends beyond shipping to markets where the use of average options is prevalent (e.g., energy commodities (Kyriakou et al., 2016), agriculturals (Geman, 2005) and metals (www.lme.com/trading/contract-types/tapos/)), as well as long-term real options with decision features on other income-generating real assets, such as plant and equipment, real estate and commodity-linked assets (e.g., oil wells, refineries, gas storage facilities).

Previously, the freight rate dynamics has been modelled by a geometric Brownian motion (e.g., see Andersen, 1992, Koekebakker et al., 2007). Nomikos et al. (2013) augmented the original model by jumps of normal size (Merton model) to account for upside jumps in the spot freight rates, due to the inability of supply to immediately respond to increased demand for seaborne trade, but also downside movements during market recessions. Mean-reverting variations by means of an Ornstein–Uhlenbeck (OU) model have also been considered in earlier communications, including Bjerksund and Ekern (1995), Alesii (2005), Sødal et al. (2008), Sødal et al. (2009) and Jørgensen and De Giovanni (2010) to name but a few, in order to describe the tendency of freight rates towards the long-run cost of transportation service provision. Nevertheless, as truly put forward by Tvedt (1997), the assumption of a Gaussian-OU process is not particularly realistic as this is not downward-restricted implying possible negative spot freight rates, especially if volatility is high (which we confirm in our analysis in Section 3.1), in addition to the resulting symmetry of freight rates while these actually appear to be skewed. These deficiencies can be alleviated by using instead a geometric mean-reverting process as in Tvedt (1997).

In the current research, we establish a generalized stochastic freight rate framework in the form of an exponential mean-reverting process overlaid with jumps of random magnitude and arrival which aims to strike a good balance between realism and level of sophis-

---

[3]In modelling the investment timing decision, we assume that investors are solely concerned about the potential profitability of their investment and thus their investment choice is not influenced by behavioural biases such as competition neglect (Greenwood and Hanson, 2015).

tication/tractability. This encompasses the geometric Brownian motion if mean-reverting variations and jumps are disallowed; the geometric mean-reverting process if jumps are excluded; the Merton model if mean-reverting variations are excluded; the Gaussian-OU process if jumps are disallowed and a logarithmic transformation is applied. The model is calibrated using cash-settled freight options with different maturities, whose payoff depends on the discrete arithmetic average of the spot Baltic Capesize Index over a predetermined time period; these are the most liquid contracts representing about 90% of the total trading volume in freight options (www.balticexchange.com).

Our in- and out-of-sample empirical analysis suggests that the postulated model with mean-reversion and jumps offers a sufficiently rich and realistic representation of the spot freight rate process. This then affects the expected cash flows from real shipping investment activities, hence provides the investors with the necessary information to make prudent investment decisions; ignoring any of these features can result in error on decision-taking[4]. To demonstrate this, we present a fair valuation setup for vessels of a given economic life cycle. Sensitivity formulae with respect to valuation inputs are also derived to infer the limits of variability of vessel values associated with changes of these inputs. For example, a critical parameter when considering an investment in a newbuilding vessel is the construction lag, which itself involves uncertainty causing delays in vessel deliveries. This implies the existence of an immediate delivery premium which is reflected in our valuation exercise, i.e., the value of a newbuilding vessel with construction lag is slightly lower than the value of a readily available five-year-old vessel; this is generally more profound during periods of prosperous market conditions and relatively full orderbook. Our results support the existence of a high investment opportunity cost embedded in the construction lag of a newbuilding vessel compared to readily available vessels. As the time-to-build declines, the investment volatility

---

[4]Negative and positive effects caused by extreme events are linked to the uncertainty of the payoff from a project, resulting into ending the investment opportunity or boosting its prospects. Similarly, mean-reversion implies that freight may temporarily be high or low but will tend towards the equilibrium freight; this is directly related to the profitability of freight-linked projects and might also have an impact on the timing of investment, depending on the speed of mean-reversion and the prevailing market conditions.

increases (Kalouptsidi, 2014) as well as the value of the option to wait. Finally, we find that the exercise time of the option increases with the vessel age.

The rest of the paper is organized as follows. Section 2 outlines the details of the postulated spot freight rate model dynamics and develops the valuation setup for traded derivatives settled on the average freight rate. Section 3 presents the outcome of the model calibration. Section 4 defines and solves the vessel valuation problem. Using our results from the previous sections, in Section 5 we develop an application in investment appraisal based on real option approach and present numerical experiments. Section 6 concludes. Several proofs and other details are deferred to the appendices.

2   Model Setup and Valuation

2.1   Market Description

Freight markets are notoriously volatile. During the period 2003–2008, freight rates for capesize drybulk carriers, with a cargo-carrying capacity of 180,000 mt dwt, increased from an average rate of 20,000 USD/day to a maximum of 236,000 USD/day only to drop to 6,000 USD/day within a period of four months after the onset of the financial crisis. Given the high volatility, it is not surprising that market participants increasingly rely on the use of forward and option contracts to manage freight rate exposure.

Forward contracts on freight, known as Forward Freight Agreements (FFAs), are cash-settled and trade the arithmetic average spot freight rate or charter hire rate for delivery at a future date. The underlying spot rate reflects the cost of hiring (chartering) a bulk carrier across a range of indicative shipping routes for the transportation of drybulk commodities and is expressed in USD/day.[5] FFAs are an effective and popular tool for hedging freight

---

[5]Spot rates are obtained using the market assessments by a panel of independent shipbrokers on the prevailing open market level for the routes defined by the Baltic Exchange and are reported by the Baltic Exchange on a daily basis. As a benchmark for the level of freight rates, the market uses the trip-charter route average of four benchmark capesize routes, known as Baltic Capesize Index 4TC (www.balticexchange.com).

rate risk. For 2015 the equivalent trading volume in FFAs has been about 640,000 cargo trading days, which is roughly equivalent to the full capacity of the underlying capesize fleet (www.balticexchange.com). Although FFAs allow traders to lock in a given freight rate over a period of time, they lack the flexibility that would enable their users to maintain the hedge in case market moved against them. Options, on the other hand, offer this flexibility.

The options market has gained popularity recently with a trading volume of 280,000 cargo days for 2015 and an average weekly open interest of 140,000 cargo trading days. In this study we consider freight options traded on the Baltic Capesize Index (BCI) as they are by far the most liquid contracts representing about 90% of the total trading volume in freight options (www.balticexchange.com). The freight options belong to the family of path-dependent contingent claims called Asian options whose payoff depends on the average price of some underlying asset (e.g., see Zhang, 1995). More specifically, the BCI freight options are settled on the arithmetic average of the spot Baltic assessments over the trading days of the settlement month. The average-based settlement procedure is inherited from the FFA market in response to concerns about the possibility of market manipulation by large participants in such a highly volatile market.

2.2 The Spot Model and the FFA Price

In what follows, we denote by S_t, $t \in [0, \infty)$, the underlying spot freight rate dynamics. We define this through $X_t = \ln S_t$ as follows:

$$X_t = Y_t + L_t, \tag{1}$$

where

$$dY_t = k(\varepsilon - Y_t)dt + \sigma dW_t, \quad Y_0 = X_0,$$

8

W is a standard Brownian motion, k is the mean-reversion coefficient that describes the rate at which process Y is expected to be pulled towards level ε, and σ is the diffusion coefficient. L is an independent compound Poisson process with a constant arrival rate of $\lambda > 0$ jumps (per unit time) of size J; J is modelled by a sequence of independent and identical normal random variables with $E(J) =: \mu_J$ and $\text{Var}(J) =: \sigma_J^2$. We call $S_t = \exp(X_t)$ the MRJ model; this includes the basic lognormal and exponential OU processes as special cases when jumps and the mean-reversion feature are ignored (we also consider these in Section 3.2). The choice of model (1) to describe the (log) spot dynamics is motivated by observed mean-reversion and existence of discontinuities in the freight market (see Section 3.1 for further discussion).

The characteristic function of (1) is given by

$$\phi_0(u;t) = E\left(e^{iuX_t}\right) = \exp\left\{ iuX_0 e^{-kt} + iu\varepsilon(1 - e^{-kt}) - \frac{\sigma^2 u^2}{4k}(1 - e^{-2kt}) + \xi(u)t \right\}, \quad (2)$$

where

$$\xi(u) := \ln E(e^{iuL_1}) = \lambda(e^{iu\mu_J - u^2\sigma_J^2/2} - 1) \quad (3)$$

is the characteristic exponent of L (e.g., see Cont and Tankov, 2004). By differentiating the cumulant generating function $\ln \phi_0(u;t)$ we obtain the cumulants

$$
\begin{aligned}
E(X_t) &= \frac{1}{i}\frac{\partial \ln \phi_0}{\partial u}(0;t) = \varepsilon + (X_0 - \varepsilon)e^{-kt} + \lambda\mu_J t, & (4) \\
\text{Var}(X_t) &= \frac{-\partial^2 \ln \phi_0}{\partial u^2}(0;t) = \frac{\sigma^2(1 - e^{-2kt})}{2k} + \lambda(\mu_J^2 + \sigma_J^2)t, & (5) \\
E\left[(X_t - E(X_t))^3\right] &= \frac{-1}{i}\frac{\partial^3 \ln \phi_0}{\partial u^3}(0;t) = \lambda\mu_J(\mu_J^2 + 3\sigma_J^2)t, & (6) \\
E\left[(X_t - E(X_t))^4\right] - 3\text{Var}^2(X_t) &= \frac{\partial^4 \ln \phi_0}{\partial u^4}(0;t) = \lambda(\mu_J^4 + 6\mu_J^2\sigma_J^2 + 3\sigma_J^4)t. & (7)
\end{aligned}
$$

Note that as t increases, the $\exp(-kt)$ term in (4) approaches zero and the expected log-spot price approaches $\varepsilon + \lambda\mu_J t$, i.e., in the long run the expected log-spot prices behave as if they started at a level ε and grow at a rate of $\lambda\mu_J$. Scale-free versions of the third and fourth

cumulants, i.e., the skewness coefficient and excess kurtosis, are given respectively by

$$\frac{E\left[(X_t - E(X_t))^3\right]}{\mathrm{Var}^{3/2}(X_t)} \quad \text{and} \quad \frac{E\left[(X_t - E(X_t))^4\right]}{\mathrm{Var}^2(X_t)} - 3. \tag{8}$$

Finally, assuming that the underlying spot price is monitored at the time points $t_0, \ldots, t_j, \ldots, t_N$ over the period $[0, T]$, we obtain the FFA price

$$F(0, t_0, t_N) = \frac{\sum_{j=0}^{N} E(S_{t_j})}{N+1} = \frac{\sum_{j=0}^{N} \phi_0(-i; t_j)}{N+1},$$

where the second equality follows from (2).

2.3 The Option Pricing Model

An option in which the average freight rate is settled against a pre-specified strike price is called an average rate (or fixed strike) option; an option in which the freight rate at the option maturity is settled against the average strike price during a specified period prior to settlement is called an average strike (or floating strike) option. In line with the market practice we consider the fixed strike type, although our approach can be adapted to the average strike type (more details can be made available by the authors upon request).

Let τ be the time of commencement of averaging and T the option maturity time. Suppose that the spot price of freight S is monitored over the period $[\tau, T]$, $T > \tau \geq 0$, at the following equidistant dates: $t_0 = \tau, \ldots, t_j = \tau + j\Delta, \ldots, t_N = T$. In addition, part of the underlying price process may be realized by the valuation date, in which case the average option is *in progress*; let $\tilde{N} + 1$ be the number of dates at which the price has already been observed and $\tilde{t} := t_{\tilde{N}} - \tau \mathbf{1}_{\{\tau > 0, \tilde{N} = 0\}}$ the option valuation date. We distinguish among three cases of practical relevance:

(a) $\tau = 0$ and $\tilde{N} = 0$ so that the time to maturity of the Asian option and the length of the averaging period coincide, i.e., both are equal to T.

(b) $\tau > 0$ and $\tilde{N} = 0$ so that averaging starts at the predetermined future time τ and is completed at T in which case we have a *forward start* option, i.e., the time to maturity of the option T is greater than the length of the averaging period $T - \tau$.

(c) $\tau \geq 0$ and $\tilde{N} > 0$ so that averaging starts at τ with part of the average being realized by the valuation date $\tilde{t}$ hence the option is in progress, i.e., the time to maturity of the option $T - \tilde{t}$ is smaller than the length of the averaging period $T - \tau$.

The terminal payoff of the arithmetic Asian option depends on the average of the $N + 1$ spot prices

$$\frac{\sum_{j=0}^{N} S_{t_j}}{N + 1}.$$

The price of the fixed strike arithmetic Asian call option is given by

$$E_{\tilde{t}}\left[e^{-r(T-\tilde{t})} \left(\frac{\sum_{j=0}^{N} S_{t_j}}{N + 1} - K \right)^+ \right] = E_{\tilde{t}}\left[e^{-r(T-\tilde{t})} \left(\frac{\sum_{j=\tilde{N}+1}^{N} S_{t_j}}{N + 1} - \tilde{K} \right)^+ \right], \tag{9}$$

where $x^+ := \max(x, 0)$, $E_{\tilde{t}}$ denotes the expectation conditional on the information available at the valuation time $\tilde{t}$,

$$\tilde{K} = K - \frac{\sum_{j=0}^{\tilde{N}} S_{t_j}}{N + 1}$$

is the excess of the fixed strike price K over the realized weighted sum of spot prices up to the valuation date, and r denotes the continuously compounded risk free rate of interest. Based on the generic identity $(x - y)^+ - (y - x)^+ = x - y$, the price of the put option is given by

$$
\begin{aligned}
&E_{\tilde{t}}\left[e^{-r(T-\tilde{t})} \left(\tilde{K} - \frac{\sum_{j=\tilde{N}+1}^{N} S_{t_j}}{\tilde{N} + 1} \right)^+ \right] \\
&= e^{-r(T-\tilde{t})} E_{\tilde{t}}\left[\left(\frac{\sum_{j=\tilde{N}+1}^{N} S_{t_j}}{\tilde{N} + 1} - \tilde{K} \right)^+ - \left(\frac{\sum_{j=\tilde{N}+1}^{N} S_{t_j}}{\tilde{N} + 1} - \tilde{K} \right) \right] \\
&= e^{-r(T-\tilde{t})} \left\{ E_{\tilde{t}}\left[\left(\frac{\sum_{j=\tilde{N}+1}^{N} S_{t_j}}{\tilde{N} + 1} - \tilde{K} \right)^+ \right] - \frac{\sum_{j=\tilde{N}+1}^{N} \phi_{\tilde{t}}(-i; t_j)}{N + 1} + \tilde{K} \right\},
\end{aligned}
$$

where the first term in the last equality is the price of the Asian call option (see Eq. 9) and from (2)

$$
\begin{aligned}
\phi_{\tilde{t}}(-i; t_j) &= E_{\tilde{t}}\left(S_{t_j}\right) \\
&= \exp\left\{ X_{\tilde{t}}e^{-k(t_j-\tilde{t})} + \varepsilon(1 - e^{-k(t_j-\tilde{t})}) + \frac{\sigma^2}{4k}(1 - e^{-2k(t_j-\tilde{t})}) + (t_j - \tilde{t})\xi(-i) \right\}.
\end{aligned}
$$

In light of the lack of analytical tractability of the law of the arithmetic average price, we additionally consider a close proxy, i.e., the arithmetic average log-price, with favourable distributional properties and explain how this can be used towards evaluating (9) of interest to us. Over any time interval $[\tau + (j-1)\Delta, \tau + j\Delta]$, $j = 1, \ldots, N$, and for the interval $[0, \tau]$ define, respectively,

$$
Z_j = X_{\tau+j\Delta} - X_{\tau+(j-1)\Delta}e^{-k\Delta}, \qquad Z_0 = X_\tau - X_0 e^{-k\tau}, \tag{10}
$$

so that from (2) $\{Z_j\}_{j=0}^N$ forms a collection of independent random variables. The characteristic function of Z_j follows from (2):

$$
\varphi(u; d) = E(e^{iuZ_j}) = \exp\left\{ iu\varepsilon(1 - e^{-kd}) - \frac{\sigma^2 u^2}{4k}(1 - e^{-2kd}) + \xi(u)d \right\}, \tag{11}
$$

where $d := \Delta$ (τ) for $1 \leq j \leq N$ $(j = 0)$. In Proposition 1, we derive a key result which represents the premise of our freight option pricing formula.

Proposition 1. *Consider Z defined in (10) with characteristic function (11). Conditional on the information available at time $\tilde{t}$, define the characteristic function of the pair $(X_{t_n}, \sum_{j=\tilde{N}+1}^N X_{t_j}/(N+1))$ for any $\tilde{N} < n \leq N$*

$$
\Psi_{\tilde{t},n}(u, v) = E_{\tilde{t}}\left[\exp\left\{ iuX_{t_n} + \frac{iv}{N+1} \sum_{j=\tilde{N}+1}^N X_{t_j} \right\} \right]. \tag{12}
$$

(i) Let $\tilde{t} = t_{\tilde{N}} = \tau + \tilde{N}\Delta \geq \tau$ (cases a and c). Then,

$$
\begin{aligned}
\Psi_{t_{\tilde{N}},n}(u,v) &= \exp\left\{ iX_{t_{\tilde{N}}} e^{-k(n-\tilde{N})\Delta} \left(u + v\frac{e^{k(n-\tilde{N})\Delta} - e^{-k(N-n)\Delta}}{(e^{k\Delta}-1)(N+1)} \right) \right\} \\
&\quad \times \prod_{j=1}^{n-\tilde{N}} \varphi\left(ue^{-(n-\tilde{N}-j)k\Delta} + v\frac{e^{k\Delta} - e^{-k(N-\tilde{N}-j)\Delta}}{(e^{k\Delta}-1)(N+1)}; \Delta \right) \\
&\quad \times \prod_{j=n-\tilde{N}+1}^{N-\tilde{N}} \varphi\left(v\frac{e^{k\Delta} - e^{-k(N-\tilde{N}-j)\Delta}}{(e^{k\Delta}-1)(N+1)}; \Delta \right).
\end{aligned}
\tag{13}
$$

(ii) Let $\tilde{t} = 0$ and $t_{\tilde{N}} = \tau > 0$, hence $\tilde{t} < \tau$ (case b). Then,

$$
\begin{aligned}
\Psi_{0,n}(u,v) &= \exp\left\{ iX_0 e^{-k\tau}\left(ue^{-(n-\tilde{N})k\Delta} + v\frac{1 - e^{-k(N-\tilde{N})\Delta}}{(e^{k\Delta}-1)(N+1)} \right) \right\} \\
&\quad \times \varphi\left(ue^{-(n-\tilde{N})k\Delta} + v\frac{1 - e^{-k(N-\tilde{N})\Delta}}{(e^{k\Delta}-1)(N+1)}; \tau \right) \\
&\quad \times \prod_{j=1}^{n-\tilde{N}} \varphi\left(ue^{-(n-\tilde{N}-j)k\Delta} + v\frac{e^{k\Delta} - e^{-k(N-\tilde{N}-j)\Delta}}{(e^{k\Delta}-1)(N+1)}; \Delta \right) \\
&\quad \times \prod_{j=n-\tilde{N}+1}^{N-\tilde{N}} \varphi\left(v\frac{e^{k\Delta} - e^{-k(N-\tilde{N}-j)\Delta}}{(e^{k\Delta}-1)(N+1)}; \Delta \right).
\end{aligned}
\tag{14}
$$

Proof. See Appendix A.1. ■

We present next an analytical approximation to the price of the Asian option (9) in the form of the lower bound

$$
\mathrm{LB}_{\tilde{t}}(l) \leq E_{\tilde{t}}\left[e^{-r(T-\tilde{t})}\left(\frac{\sum_{j=\tilde{N}+1}^{N} S_{t_j}}{N+1} - \tilde{K} \right)^+ \right],
$$

where

$$
\mathrm{LB}_{\tilde{t}}(l) := E_{\tilde{t}}\left[e^{-r(T-\tilde{t})}\left(\frac{\sum_{j=\tilde{N}+1}^{N} S_{t_j}}{N+1} - \tilde{K} \right) \mathbf{1}_{\left\{ \frac{1}{N+1}\sum_{j=\tilde{N}+1}^{N} X_{t_j} > l \right\}} \right].
\tag{15}
$$

The idea of such a bound dates back to the seminal contributions of Curran (1994) and Rogers and Shi (1995) which are, nevertheless, restricted to basic lognormal asset price dy-

namics. Their exposition is incomplete leaving unattainable various modelling processes including, for example, mean-reverting features and price discontinuities, which are important for commodity markets, and contract-specific features such as forward-start and in-progress averaging. In addition to recent research work by Fusai and Kyriakou (2016), our current contribution removes the remaining block to universal application solving a long-standing pricing problem by optimization[6]. In Theorem 2, we tailor to our log-spot freight model (1) and freight option design described at the beginning of this section (cases a–c) and show how to evaluate (15) using our results in Proposition 1. Finally, we note that our approach can be easily adapted to alternative model specifications, requiring only knowledge of the characteristic function of the driving process (see Proposition 1), while remaining highly precise to 4 decimal places[7].

Theorem 2. *The optimal price lower bound is given by*

$$\mathrm{LB}_{\tilde{t}}(l^*) = \frac{e^{-\delta l^*}}{2\pi} \int_{\mathbb{R}} e^{-iul^*} \Phi_{\tilde{t}}(u) du, \tag{16}$$

where

$$\Phi_{\tilde{t}}(u) = \frac{e^{-r(T-\tilde{t})}}{iu + \delta} \left(\frac{1}{N+1} \sum_{j=\tilde{N}+1}^{N} \Psi_{\tilde{t},j}(-i, u - i\delta) - \tilde{K}\Psi_{\tilde{t},N}(0, u - i\delta) \right) \tag{17}$$

is the Fourier transform of (15) with respect to l, constant $\delta > 0$ ensures integrability, $\Psi_{\tilde{t},j}$ is given by (13) or (14), and

$$l^* := \arg\max_l \mathrm{LB}_{\tilde{t}}(l) \tag{18}$$

satisfies the optimality condition

$$E_{\tilde{t}} \left(\frac{\sum_{j=\tilde{N}+1}^{N} S_{t_j}}{N+1} \middle| \frac{\sum_{j=\tilde{N}+1}^{N} X_{t_j}}{N+1} = l^* \right) = \tilde{K}. \tag{19}$$

---

[6]A thorough survey of previous pricing attempts is beyond the scope of this paper; we refer, for example, to Fusai and Kyriakou (2016) for more details.

[7]We felt that presenting speed-accuracy tradeoffs against true (but time-consuming) Monte Carlo price estimates indicating the substantial numerical gain of our method was beyond the scope of this paper, however we can make them available upon request.

Proof. See Appendix A.2. ∎

3 Model Calibration and Analysis

We calibrate the MRJ spot freight model for the capesize sector of the drybulk market
using Baltic Option Assessments (BOAs). These are market assessments of at-the-money
option implied volatilities submitted to the Baltic Exchange by freight option brokers, with
strikes equal to the prevailing FFA rates which we collect also from the Baltic Exchange. We
consider options with different maturities on every Friday in the period 04 January 2008 to
27 June 2014, i.e., a total of 339 weeks. Conforming to market practice, we use the implied
volatilities as input in the pricing formula of Turnbull and Wakeman (1991) and Levy (1997)
(discrete average) to recover the market quotes of BCI Asian call options for the next four
quarters (+1Q, +2Q, +3Q and +4Q) and the next two calendar years (+1CAL and +2CAL).
Each quarterly contract consists of three options that expire at the end of each month in
the relevant quarter, whereas a calendar contract is a strip of twelve monthly options. The
settlement prices of the options are given by the average spot rates over the trading days of
the settlement month. For example, on 04 January 2014, the +1Q contract comprises three
options which settle at the end of April, May, and June 2014; the first option is based on the
average spot rate in April, the second corresponds to May and the third to June. Succinctly,
our dataset comprises 36 at-the-money options with different maturities on each week in
our sample, yielding a total of 12,204 option prices. We also collect information about the
spot BCI as at the valuation date of each option during our sample period from the Baltic
Exchange. Spot interest rates are available from the Datastream.

We extract risk neutral parameter estimates of the MRJ model from observed option
prices. More specifically, let P^M and P^θ be, respectively, the market option price and
the theoretical option price under the log-spot rate model (1) with parameter vector $\theta :=
\{k, \varepsilon, \sigma, \lambda, \mu_J, \sigma_J\}$. Theoretical option prices are computed fast via the formula (16) by

quadrature in Matlab (up to 5 seconds per price) and at high accuracy (4 decimal places). We estimate θ every week $w = 1, \ldots, 339$ in our sample by minimizing the in-sample quadratic pricing error (e.g., see Bates, 1996, Bakshi et al., 1997, Hilliard and Reis, 1999, Andersen and Andreasen, 2000) across option maturities

$$\theta_w^* := \arg\min_{\theta_w} \sum_{i=1}^{m} \left| P_{i,w}^M - P_{i,w}^{\theta_w} \right|^2, \tag{20}$$

where $m = 36$ is the number of maturities. The minimization problem (20) is solved by standard nonlinear least-squares solver in Matlab.

3.1   Parameter Estimates and Market Behaviour

The estimated parameters of the BCI MRJ model are presented in Panel A of Table 1. In particular, we report the averages of the implied annual parameter values obtained across the weeks in the sample period along with their standard errors. Several comments are in order. The estimated degree of mean-reversion k is 3.310, implying that it takes an average of 2.5 months for the log-spot rate to return half way towards the long-run level ε (half-life is computed as $\ln 2^{1/k}$). Mean-reversion in the shipping markets is justified on the basis that high freight rates encourage investment in new capacity, which increases future supply and subsequently lowers freight rates. On the other hand, low freight rates result in reduction in operating performance and divestment either in the form of laying-up vessels or even scrapping; the combined effect is a reduction in the supply of services and an increase in the level of freight rates. Mean-reversion in freight rates is also observed in the volatility term structure of forward contracts as longer maturity contracts, in general, tend to have lower volatility than short-term ones as noted in Nomikos et al. (2013).

Consistent with the volatile nature of the shipping industry, the annualized volatility σ of diffusive shocks is high at 68.8%. In shipping markets, the supply of services is perfectly elastic at low levels of utilization, but as fleet utilization increases the supply schedule turns

inelastic. In other words, when demand is strong and the available fleet is fully utilized, a positive (negative) demand shock[8] leads to a relatively larger upward (downward) price movement. Abrupt adjustments in prices can be captured by the jump component of the MRJ model. The estimated expected number of jumps per year λ is 6.786, and the mean jump size μ_J is -27.2% in consistency with the observed negative skewness in historical freight rates which may be indicative of an asymmetric response to good and bad news (leverage effect). Spot freight rates may also exhibit relatively large upside movements due to the inability of supply to immediately respond to changes in demand due to the construction lag inherent in shipbuilding. However, it seems that upside movements are less marked than downside movements. In other words, as the rate of fleet utilization increases, we anticipate rising freight rates with a certain degree of persistence; on the other hand, price decreases, mostly linked to a reduction in economic activity, consumption rates or changes in geographical demand are more pronounced. For example, during the 2008 market recession, we evidenced an 80% average decrease in the freight rates in the course of only 4 months. It is also interesting to note that over the period 2008–2014, the growth in fleet size outpaced the growth in demand (seaborne trade), as shown in Figure 1, which caused abrupt downward freight rate movements. The resulting excess capacity meant that increases in demand could be easily absorbed, while reductions in demand meant that freight rates stayed at lower levels for longer periods of time.

We conclude this part by presenting in Figure 2 the weekly evolutions of the implied volatility, skewness and excess kurtosis of the 1-week, 1-month and 1-year log-changes in the BCI computed using (5) and (8). The skewness is negative consistent with the negative mean jump size. Increasing the time scale results in higher volatility, whereas excess kurtosis decreases and skewness increases towards zero as the jump effect dies out.

---

[8]Such shocks can be due to a number of factors: seasonal fluctuations in demand, such as a reduction in industrial activity in China before the Chinese new year or the slowdown of industrial activity in Europe during the summer months; changes in harvest expectations for agricultural commodities; changes in market expectations and unanticipated macroeconomic developments; political events; hurricane disruptions in port facilities; port congestion; and temporary supply-demand imbalances.

3.2 Robustness Checks

To formally test the accuracy of the fitted MRJ model, we calculate the weekly mean absolute percentage error

$$\text{MAPE}_w = \frac{1}{m} \sum_{i=1}^{m} \left| 1 - \frac{P_{i,w}^{\theta_w^*}}{P_{i,w}^M} \right| \tag{21}$$

and the root mean square percentage error

$$\text{RMSPE}_w = \sqrt{\frac{1}{m} \sum_{i=1}^{m} \left| 1 - \frac{P_{i,w}^{\theta_w^*}}{P_{i,w}^M} \right|^2}, \tag{22}$$

where θ_w^* is given by (20). Panel B of Table 1 presents the average error statistics obtained across the weeks in the sample period. Both in- and out-of-sample pricing error statistics are reported.

In addition to the whole set of option pricing errors, which we label "All options", we report the results of three subsets comprising short, medium and long-term options: the first subset is the +Q which encompasses the quarterly contracts with maturities up to the next four quarters, i.e., +1Q, +2Q, +3Q, +4Q; the second subset includes the calendar options with maturities between 13 and 24 months (+1CAL); and the third one maturities between 25 and 36 months (+2CAL). For the dataset "All options", in-sample MAPE and RMSPE are 11.91% and 16.99%, respectively. For the maturity-partitioned subsets, the pricing errors improve in the case of longer-term contracts as the short-end of the forward curve, which is relatively sensitive to information arrival (Samuelson (1965) effect), puts more stress on the pricing experiments. To validate the model and study whether or not it over-fits the option prices during the in-sample period, we perform out-of-sample pricing of options one week ahead using our weekly in-sample estimates; we find that out-of-sample pricing errors do not deviate significantly from the in-sample results. Finally, we use the stationary bootstrap of Politis and Romano (1994) to test the null hypothesis of the MRJ not performing better than

a benchmark model[9]. As benchmarks, we consider the exponential mean-reverting model without jumps (MR) and the basic lognormal (LogN) model which we calibrate on the same dataset. We find that MRJ improves on MR and LogN models across all maturities at the 1% significance level.

Systematic bias from uncaptured factors is likely to be associated with the percentage in-sample/out-of-sample pricing errors $\text{PE} = (P^{\theta^*} - P^M)/P^M$. Following Bakshi et al. (1997) and other authors, we investigate this by estimating regressions of the type

$$\text{PE}_w = \beta_0 + \beta_1 T_w + \beta_2 T_w^2 + \beta_3 \hat{\sigma}_{S,w}^2 + \beta_4 dy_w + u_w, \tag{23}$$

where T is the option's time to maturity measured in years, T^2 accounts for a nonlinear time-to-maturity effect (option-specific variables), $\hat{\sigma}_S$ is the annualized 6-month rolling standard deviation of the spot freight rate S (shipping sector-specific) and dy the yield differential between the 30-year and 3-month US T-bill rates (general market conditions). Based on the reports in Table 2, the mean error under the MRJ model is negative and statistically significant, implying that the model tends to underprice options. The coefficients of T and T^2 are significant with positive and negative sign, respectively, implying a concave relationship of the error with T. The coefficients of $\hat{\sigma}_S^2$ are found insignificant. The yield differential movements have a significant positive effect on the PE, i.e., accounting for interest rate movements can lead to pricing improvement albeit small. The F-statistic suggests that the joint effect of the independent variables is statistically significant, however the overall impact on the pricing bias appears to be relatively small with the adjusted in-sample (out-of-sample) R^2-statistic being only 1.73% (1.31%). On the contrary, as suggested by the adj. R^2 and F-statistics, the option prices resulting from the elementary MR and LogN models are more prone to systematic errors.

---

[9]We define loss functions between the benchmark (MR or LogN) and the MRJ model error statistics, e.g., $\text{LF} = \text{MAPE}_{\text{MRJ}} - \text{MAPE}_{\text{benchmark}}$. Then, using 10,000 bootstrap simulations, we test the null hypothesis that the benchmark cannot be outperformed by the MRJ model. For more details, we refer to Politis and Romano (1994) and Sullivan et al. (1999, Appendix C).

Overall, we conclude that modelling mean-reversion and jumps results in a richer and more realistic representation of the spot freight rate. In Sections 4 and 5, we present two important applications of the proposed model and contributions of this research in ship valuation and investment appraisal.

4 Model Application to Real Assets: Vessel Valuation

In what follows, we present a fair valuation framework for vessels of a given economic life cycle. Sensitivity formulae with respect to valuation inputs are also derived to infer the limits of the variability for the vessel value. In this and the next section, operating profits are assumed to evolve according to the MRJ model of Section 2.2. Fair vessel values are computed based on the parameter estimates in Table 1. Unless otherwise stated, the following assumptions apply: initial spot freight rate of 34,700 USD (spot BCI 4TC), scrap price of 9.5 million USD for a capesize vessel and interest rate of 3.9% per annum (30-year US Treasury bond); these values represent average historical market quotes over the estimation period. We also assume that there are no taxes and that a typical vessel has an economic life of 25 years while, once operation starts, the vessel is on-hire 348 days per year (the remaining 17 days represent time off-hire for maintenance). We consider readily available newbuildings (no construction lag) and vessels with an order-delivery gap (construction lag) of two years, as well as 5Y, 10Y, 15Y and 20Y secondhand vessels. All shipping-related data are from the Clarkson Shipping Intelligence Network; interest rates are from the Datastream.

4.1 The Value of a Vessel

Let $l \geq 0$ be the construction lag of a newbuilding (NB) vessel (if applicable), $\bar{T} \in \{5, 10, 15, 20, 25\}$ the remaining ship life, and $\bar{V}$ the vessel scrap value.

Proposition 3. *The ship value V at time $t \geq 0$ is given by*

$$
\begin{aligned}
V(t, \bar{T}) &= E_t \left[\int_{t+l}^{t+l+\bar{T}} e^{-r(w-t)} S_w dw \right] + \bar{V} e^{-r(\bar{T}+l)} \\
&= \int_{t+l}^{t+l+\bar{T}} e^{-r(w-t)} \phi_t(-i; w) dw + \bar{V} e^{-r(\bar{T}+l)},
\end{aligned}
\tag{24}
$$

where E_t denotes the expectation conditional on the information available at time t,

$$
\begin{aligned}
\phi_t(u; w) &= E_t \left(e^{iuX_w} \right) \\
&= \exp \left\{ iuX_t e^{-k(w-t)} + iu\varepsilon(1 - e^{-k(w-t)}) - \frac{\sigma^2 u^2}{4k}(1 - e^{-2k(w-t)}) + (w-t)\xi(u) \right\}
\end{aligned}
$$

and ξ is given by (3).

Proof. Follows from Fubini's theorem. ∎

Table 3 reports our valuation results. The value of the NB with no construction lag is the highest, whereas if we assume a construction lag of 2 years the value decreases. Further, the value of the NB with construction lag is slightly lower than that of a 5Y vessel. This can be attributed to the immediate delivery premium during periods of prosperous freight market conditions and relatively full orderbooks, as was the case of the drybulk market during 2006–2008. The term structure of vessel values is negatively sloped and concave. For example, the difference between a readily available NB and a 5Y vessel is 6.5 million USD, whereas the difference between a 15Y and a 20Y vessel exceeds 13.5 million USD. This possibly implies mild depreciation in the first years of operation, while as vessels approach the end of their economic life the price differential becomes wider before their values level off at scrapping.

Figure 3 (top-left sub-figure) exhibits the model values of capesize vessels of different ages along with the corresponding historical mean values and 5th and 95th percentiles for the entire sample (January 2008–June 2014). The remaining sub-figures exhibit the model relative to the historical mean values for each year in our sample across different vessel ages. We find that model-implied vessel values track mean market quotes well, both over the entire

and yearly-partitioned sample period. The average difference is about 25% but this varies with vessel age; it is very small for a NB (0.16%) and relatively young vessels (e.g., 7.49% for a 5Y) and increases with vessel age. This can be attributed to the fact that vessels spend more time off-hire and may also command lower freight rates as their age increases. Given that the buyer and seller are cognisant of the market and face no compulsion to act, any discrepancy between model-implied and market prices may be due to an expected revenue based on an index/route other than the BCI, a different scrap value or life cycle.

Having set up the valuation model, by differentiating (24) under the integral sign, we derive first-order partial sensitivities of the theoretical vessel values with respect to various valuation inputs of interest, i.e., scrap price $\bar{V}$, interest rate r, long-run freight rate $\exp(\varepsilon)$, diffusion coefficient σ, speed of mean-reversion k and jump arrival rate λ:

$$
\frac{\partial V(t,\bar{T};\bar{V})}{\partial \bar{V}} = e^{-r(l+\bar{T})}, \tag{25}
$$

$$
\frac{\partial V(t,\bar{T};r)}{\partial r} = -\int_{t+l}^{t+l+\bar{T}} e^{-r(w-t)}(w-t)\phi_t(-i;w)dw - (\bar{T}+l)\bar{V}e^{-r(\bar{T}+l)}, \tag{26}
$$

$$
\frac{\partial V(t,\bar{T};\varepsilon)}{\partial e^{\varepsilon}} = \int_{t+l}^{t+l+\bar{T}} e^{-r(w-t)-\varepsilon}\left(1 - e^{-k(w-t)}\right)\phi_t(-i;w)dw, \tag{27}
$$

$$
\frac{\partial V(t,\bar{T};\sigma)}{\partial \sigma} = \int_{t+l}^{t+l+\bar{T}} e^{-r(w-t)}\frac{\sigma}{2k}\left(1 - e^{-2k(w-t)}\right)\phi_t(-i;w)dw, \tag{28}
$$

$$
\frac{\partial V(t,\bar{T};k)}{\partial k} = \int_{t+l}^{t+l+\bar{T}} e^{-r(w-t)}\left[(\varepsilon - X_t)(w-t)e^{-k(w-t)}\right.
$$
$$
\left. +\frac{\sigma^2}{4k^2}((2k(w-t)+1)e^{-2k(w-t)} - 1)\right]\phi_t(-i;w)dw, \tag{29}
$$

$$
\frac{\partial V(t,\bar{T};\lambda)}{\partial \lambda} = \int_{t+l}^{t+l+\bar{T}} e^{-r(w-t)}(w-t)(e^{\mu_J+\sigma_J^2/2} - 1)\phi_t(-i;w)dw. \tag{30}
$$

Results are presented in Table 3. Price sensitivities (26)–(30) increase as vessel age decreases. An exception is the sensitivity with respect to the scrap price $\bar{V}$ (25) due to the impact of discounting: a 1 million USD change in $\bar{V}$ causes a change of 0.376 million USD in the price of the NB ($l = 0$). This effect becomes stronger as vessels approach demolition since, as time passes, $\bar{V}$ represents a larger proportion of the vessel's total value. So far,

we have assumed a constant interest rate r of 3.9% per annum. Increasing r by 1 basis point decreases the price of the NB ($l = 0$) by 72,000 USD; this effect is less pronounced in the case of secondhand vessels, e.g., a 20Y vessel whose price decreases by 9,000 USD. The interest rate effect becomes more profound when we consider larger movements in interest rates: if r rises, say, to 5%, the NB vessel values decrease to 60.2 ($l = 0$) and 52.5 ($l = 2$), and 55.6, 49.0, 40.1 and 27.9 million USD for 5Y, 10Y, 15Y and 20Y vessels, respectively. Further, we notice that vessel values rise with $\exp(\varepsilon)$ and σ and associated effects on the mean and variance of the log-freight distribution (see Equations 4–5). For example, a change in $\exp(\varepsilon)$ of 100 USD causes a substantial change in the NB ($l = 0$) price of 0.518 million USD due to fast mean-reversion (half-life of 2.5 months). On the contrary, increasing λ has a downward effect on the vessel value. For example, increasing λ by an average of 0.5 jump per year decreases the NB ($l = 0$) price by 0.441 million USD due to negative skewness of the log-freight distribution (see Figure 2). In addition, increasing k, i.e., accelerating mean-reversion, reduces the variance of the log-freight distribution (see Equation 5) and, consequently, the vessel value.

Typically, time to build involves uncertainty because actual construction duration may be affected by dock capacity constraints which may further cause delay in vessel deliveries. For this, we consider the NB vessel value sensitivity with respect to the construction lag l:

$$\frac{\partial V(0, \bar{T}; l)}{\partial l} = e^{-r(l+\bar{T})}\phi_0(-i; l + \bar{T}) - e^{-rl}\phi_0(-i; l) - r\bar{V}e^{-r(\bar{T}+l)}.$$

Deviating from the original 2-year construction lag has a perceptible effect on the vessel value. Based on the report in Table 3, an increase of the construction duration by 3 months, i.e., from 2 to to 2.25 years, decreases the price of the vessel by 0.725 million USD suggesting a higher delivery premium. This is expected as the supply of vessels is elastic only in the long run. However, even in the long run, the incentive to build is not strong as a positive demand shock eventually fades away under mean-reverting freight rates. Therefore, vessels

of forward delivery are not able to take advantage of the temporary high freight rates, driving their price to lower levels compared to vessels that are readily available in the resale market.

Finally, we investigate the impact of a change in the initial spot freight level S_0 by computing

$$\frac{\partial V(0, \bar{T}; X_0)}{\partial S_0} = \int_l^{l+\bar{T}} e^{-(r+k)w - X_0} \phi_0(-i; w) dw.$$

The impact of S_0 on vessel values is found to be of a rather small scale compared to that of $\exp(\varepsilon)$, i.e., an equivalent change in the vessel value of approx. 0.5 million USD requires a change in S_0 in excess of 7,500 USD, due to fast mean-reversion. Figure 4 depicts how vessel values vary with S_0 for given $\exp(\varepsilon)$, $\ln 2^{1/k}$, σ and λ. We observe that varying S_0 has a marginal effect on the vessel values: increasing S_0 by, say, 1,500% from 5,000 to 80,000 USD increases the vessel value by 7.96% under the original parameter estimates in Table 1 (see dotted lines). By perturbing each of ε, σ and λ (see solid lines), we observe that the sensitivity remains relatively firm and low: an increase in S_0 of 1,500% increases the vessel value by 7%-9%. Instead, varying k (hence, the half-life) makes the impact of S_0 more prominent: for a half-life of 12 months (2-5 years) a 1,500% increase in S_0 is associated with a 37% (70%-160%) increase in the vessel values.

5 The Option to Invest: An Illustrative Real Option Application

Studies have shown that the conventional NPV method fails to accurately capture uncertainty in a dynamic environment (e.g., see Dixit and Pindyck, 1994, Schwartz and Smith, 2000). To this end, in this section, we demonstrate the practicality of our real asset valuation approach in investment appraisal in the newbuilding and sale and purchase markets for vessels from a real option perspective. Our aim is to integrate the effect of stochastic cash

24

flows and the true American option nature of the investment. We consider three hypothetical investments in vessels:

(1) The firm owns the right to order and get delivery of a NB and can exercise this option at any time within the next 10-year period[10]. The NB price is 60.17 million USD (see Table 3) and there is a 2-year construction lag from the time the investment decision is made until delivery and commencement of regular operations. The initial freight rate is 34,700 USD per day and thereafter it evolves stochastically according to the MRJ model.

(2) The firm owns the right to purchase a NB in the resale market (no construction lag) and can exercise this option at any time within the next 10 years. It costs 68.04 million USD to purchase the vessel and operation starts immediately at an initial freight rate of 34,700 USD per day.

(3) The firm owns the right to purchase a secondhand vessel in the sale and purchase market and can exercise this option at any time within the next 10 years. Operation starts immediately at an initial freight rate of 34,700 USD per day. Here, we consider four different scenarios: the acquisition of a 5Y, 10Y, 15Y and 20Y vessel at a cost of 61.54, 53.21. 42.53 and 28.84 million USD, respectively.

5.1 Option to Buy a Vessel Formulation

Let T be the expiration date of an option to buy a ship with remaining lifetime $\bar{T}$. We consider an American option whose payoff to the holder on exercise at any stopping time $\tau \in [t, T]$ is given by

$$\psi(\tau; X_\tau) = (V(\tau, \bar{T}; X_\tau) - K)^+,$$

---

[10]An infinite horizon may be considered, instead, as in Schwartz and Smith (2000); for practical reasons, we assume a finite horizon here.

where K denotes the exercise price (acquisition cost of the vessel). The option fair value is the solution to the classical optimal stopping problem, namely to find the stopping time that maximizes the conditional expectation of the discounted payoff over exercise strategies:

$$g(t; X_t) = \sup_{\tau \in [t,T]} E_t \left[e^{-r(\tau-t)} \psi(\tau; X_\tau) \right]. \tag{31}$$

Unlike an American option that can be exercised at any time prior to the option's maturity, a Bermudan option can be exercised only at a discrete set of monitoring times $\mathcal{T} = \{t_j\}_{j=0}^N$ where $t_j = t + j\Delta$, $j = 0, 1, \ldots, N$, and $t_N = T$. The valuation of Bermudan options corresponds to solving a discrete optimal stopping problem with the supremum in (31) taken over the set of possible stopping times which take values in $\mathcal{T}$. The optimal stopping problem can be solved in a finite time horizon by backward induction where at each monitoring time we take the maximum between the conditional expectation, representing the continuation value of the option, and the option payoff from immediate exercise; the continuation and stopping regions are separated by a critical value. More specifically, we employ the following backward induction:

$$g(T; X_T) = \psi(T; X_T), \tag{32}$$

$$
\begin{aligned}
g(t_j; X_{t_j}) &= \max \left\{ \psi(t_j; X_{t_j}), c(t_j; X_{t_j}) \right\}, \quad 0 \le j \le N-1, &\text{(33)} \\
c(t_j; X_{t_j}) &= E_{t_j} \left[e^{-r\Delta} g(t_{j+1}; X_{t_{j+1}}) \right], \quad 0 \le j \le N-1. &\text{(34)}
\end{aligned}
$$

Denote by $m_{t_j}^*$ the value of X_{t_j} where $\psi(t_j; X_{t_j})$ and $c(t_j; X_{t_j})$ cross: for $X_{t_j} > m_{t_j}^*$, we have that $g(t_j; X_{t_j}) = \psi(t_j; X_{t_j})$, i.e., option is exercised early; instead, for $X_{t_j} < m_{t_j}^*$, we have that $g(t_j; X_{t_j}) = c(t_j; X_{t_j})$, i.e., we continue holding the option. At maturity (i.e., for $j = N$), m_T^* solves $V(T, \bar{T}; m_T^*) = K$ and the option is exercised if it ends up ITM, otherwise it is left to expire. The relevant equations can be solved numerically (see Appendix B.1).

Finally, by exploiting smooth monotone convergence of the chosen approach with increasing N, we can then obtain accurate American option prices through extrapolation via standard Richardson-type procedure.

The dynamic programming problem (32)–(34) is solved as follows. We write (34) as

$$\tilde{c}(t_j; xe^{-k\Delta}) = \int_{-\infty}^{\infty} e^{-r\Delta} g(t_{j+1}; y) f(y|xe^{-k\Delta}; \Delta) dy,$$

where f denotes the density function describing the transition from $X_{t_j} = x$ at t_j to $X_{t_{j+1}} = y$ at t_{j+1}. From the form of (2) we conclude that $f(y|xe^{-k\Delta}; \Delta) = f(y - xe^{-k\Delta}; \Delta)$, hence by changing variables we get

$$\tilde{c}(t_j; xe^{-k\Delta}) = \int_{-\infty}^{\infty} e^{-r\Delta} g(t_{j+1}; z + xe^{-k\Delta}) f(z; \Delta) dz. \tag{35}$$

Given

$$c(t_j; y) = \tilde{c}(t_j; ye^{-k\Delta}), \tag{36}$$

we get from (33)

$$g(t_j; y) = \max\{\psi(t_j; y), c(t_j; y)\}. \tag{37}$$

Recursion (35) starts as

$$\tilde{c}(t_{N-1}; xe^{-k\Delta}) = \int_{m_T^* - xe^{-k\Delta}}^{\infty} e^{-r\Delta} (V(T, \bar{T}; z + xe^{-k\Delta}) - K) f(z; \Delta) dz$$

based on the terminal condition (32). Ultimately, the option price at inception is given by $g(t_0; X_{t_0})$.

Note that evaluating f directly can be time-consuming. Instead, by exploiting knowledge of the associated characteristic function $E[\exp(iu(X_{t_{j+1}} - X_{t_j} e^{-k\Delta}))]$ from (2) and the convolution structure (35) we are able to compute the above backward induction fast and accurately by discrete Fourier transform the way we describe in Appendix B.1.

27

Remark 4. *In case exercise is only possible at the expiration date T, the option is European and the recursive solution algorithm reduces to a single backward time step from T to t.*

Remark 5. *In addition to the option price, the price sensitivities with respect to parameters of interest, e.g., the initial spot rate, can be obtained with essentially no additional computational cost by differentiating (35) under the integral sign.*

5.2   Comparison of Investment Decisions

Figure 5 portrays the NPV profiles of the hypothetical investments (1)–(3), described at the beginning of Section 5, as a function of the long-run level $\exp(\varepsilon)$ (in 000s USD) and the diffusion coefficient σ. In particular, we perturb parameters $(\exp(\varepsilon), \sigma)$ from their original values in Table 1 to obtain 825 pairs of parameter values and compute optimal exercise policies by solving the American option pricing problem described in Section 5.1 for a 10-year horizon. The dark upper surfaces depict the value of the projects under the optimal exercise policy. The white lower surfaces show the value of the projects as if immediate exercise was forced. Note that dark upper surfaces fade as the two value surfaces approach each other and become white when they overlap, i.e., regions where immediate exercise is the optimal strategy. Grey surfaces represent the zero plane as a point of reference.

We find that both parameters have an impact on the timing of the decision and value of the investment, and this impact diminishes with the vessel age as the surfaces become flatter for older vessels. More specifically, we detect a positive relationship between the two parameters and the value of the investment, i.e., NPVs increase with the parameter values. This effect is more prevalent in the case of NBs. In terms of the optimal exercise policy, the results confirm the higher delivery premium attached to readily available vessels as the optimal exercise strategy for a NB with construction lag almost always implies immediate exercise of the option to invest. Therefore, construction lag comes at a high investment opportunity cost, and delaying the investment does not add value. In contrast, it is optimal to delay the investment in a vessel that is readily available in the market unless $\exp(\varepsilon)$ and/or

σ are high. For example, consider the case of a NB in the resale market and a low value for σ of 40%; then, for any $\exp(\varepsilon) < 13,000$ USD the optimal exercise strategy suggests to wait for either σ and/or $\exp(\varepsilon)$ to increase. Similarly, the optimal exercise strategy suggests to delay the investment for values of $\exp(\varepsilon) < 11,500$ USD as long as $\sigma < 120\%$.

In general, decisions based on the conventional versus real option NPV do not differentiate for relatively high values of $\exp(\varepsilon)$ and σ, i.e., both approaches indicate immediate acquisition of the vessel then; yet, the older the vessel, the higher these values have to be for the two approaches to converge. By neglecting the value of management flexibility the conventional NPV consistently understates the investment profitability, whereas the real option strategy accounts for the strategic value of undertaking the project at some future time (even if immediate investment is not viable). Therefore, failing to consider the embedded option value leads to rejection of investment opportunities with profit potential. It is also worth noting that the real option NPVs are more conservative in terms of the "trigger" parameters for going ahead with the investment than the conventional NPVs, reflecting the risk-averse thinking of decision-makers. In effect, by accepting a marginally positive NPV, project investors lose all value from the investment timing option. This implies that real option NPV leads to a more reliable approach for making strategic high capital intensive decisions, i.e., marginally positive NPVs would not suffice to justify undertaking such a capital intensive project.

While the NPVs provide an indication of the investment's profitability, it is also useful to examine the distribution of the optimal option exercise time. To this end, for each pair of parameters $\exp(\varepsilon)$ and σ, we simulate 10,000 optimal exercise times using the least-squares Monte Carlo approach of Longstaff and Schwartz (2001) and estimate the mean optimal exercise time. Figure 6 depicts the distribution of the mean optimal exercise time for 825 pairs, from which we observe that this increases with the vessel age and that left skewness becomes more prominent. Further, the dispersion of the exercise time distribution becomes smaller with increasing vessel age due to less cash flow uncertainty for shorter remaining

economic lives.

We conclude this analysis by now focusing on the original parameter estimates in Table 1. In Table 4, we present the distributional properties of the optimal exercise time corresponding to the particular parameter set. Consistent with our earlier observation, the mean exercise time is substantially small (less than two months) for NBs with a 2-year construction lag. For NBs with no construction lag and secondhand vessels, the mean exercise time rises to 2.084-2.440 years; across the different vessel ages, the estimated probability of the exercise time to exceed 1 year ranges from 37% to 43%, whereas the probability that this lies between 1-4 or 4-7 or exceeds 7 years is 12%-14% depending on the vessel age. As before, our results corroborate the high investment opportunity cost embedded in the construction lag of a NB compared to readily available vessels and there is some evidence of increasing exercise time with the vessel age.

6   Conclusions

Investment timing and uncertainty are critical issues when committing to a capital intensive project. We develop a valuation framework for real assets which is well-suited for analyzing investment projects where income uncertainty is driven by mean-reverting variations and jumps of random magnitude and arrival.

In this paper, we use data on freight-related drybulk shipping assets to investigate empirically the stochastic nature of income and the effect of uncertainty on vessel valuation and investment decision. We find that it takes 2.5 months for the spot rate to return half way towards the long-run level. Moreover, spot freight rates exhibit abrupt movements which are mainly attributed to the inability of supply to immediately respond to changes in demand due to the construction lag inherent in shipbuilding. En masse, our results suggest that the postulated spot freight model captures flexibly the drybulk market behaviour, providing significant in- and out-of-sample assessment gains compared to benchmarks. This has

implications in derivatives pricing and capital budgeting decisions, as failing to account for mean-reversion and price discontinuities can lead to large errors and systematic biases.

To demonstrate the significance of the option value in the investment decision, we develop first a fair valuation paradigm for vessels and examine the effects of input uncertainties by means of a sensitivity analysis. We present evidence for vessels of different economic lives and find that vessel value sensitivities are higher for younger vessels. In addition, existing construction lags in the shipbuilding process may put a significant downward pressure on newbuilding vessel prices to the extent that a relatively new secondhand vessel may cost more (immediate delivery premium). We then study the NPV profiles of different investments using a real option approach and explore the optimal timing of entry. We find that long-run freight rate and volatility have an impact on the timing of the decision and value of the investment; this impact diminishes with increasing vessel age. Moreover, we observe that, as time-to-build declines, the value of the option to wait increases implying a high opportunity cost embedded in the investment decision due to construction lags.

Our work is of potential interest to various stakeholders in the industry, including investors (shareholders or private equity investors) for evaluating their prospective investment projects; providers of credit (banks or bond investors) for imposing covenants either on the mortgage of the asset or the bond issue offered by the company; regulators, as the fair value of vessels should also be reported in any investment prospectus (initial or secondary public offering, bond offering) for due diligence and accounting purposes; and governmental organizations for assessing and comparing alternative investments.

Appendix A: Proofs

A.1   Proof of Proposition 1

Proof. From (10) we get by recursive substitution that

$$X_{t_j} = X_{t_{\tilde{N}}} e^{-k(j-\tilde{N})\Delta} + \sum_{m=1}^{j-\tilde{N}} Z_m e^{-(j-\tilde{N}-m)k\Delta}, \qquad j \geq \tilde{N}+1. \tag{A.1}$$

Furthermore,

$$
\begin{aligned}
\sum_{j=\tilde{N}+1}^{N} X_{t_j} &= \sum_{j=1}^{N-\tilde{N}} \left\{ X_{t_{\tilde{N}}} e^{-kj\Delta} + \sum_{m=0}^{N-\tilde{N}-j} Z_j e^{-km\Delta} \right\} \\
&= X_{t_{\tilde{N}}} \frac{1 - e^{-k(N-\tilde{N})\Delta}}{e^{k\Delta} - 1} + \sum_{j=1}^{N-\tilde{N}} Z_j \frac{e^{k\Delta} - e^{-k(N-\tilde{N}-j)\Delta}}{e^{k\Delta} - 1}.
\end{aligned} \tag{A.2}
$$

From (A.1)–(A.2) and for $\tilde{N} < n \leq N$

$$
\begin{aligned}
&\exp\left\{ iuX_{t_n} + \frac{iv}{N+1} \sum_{j=\tilde{N}+1}^{N} X_{t_j} \right\} \\
&= \exp\left\{ iuX_{t_{\tilde{N}}} e^{-k(n-\tilde{N})\Delta} + iu \sum_{m=1}^{n-\tilde{N}} Z_m e^{-(n-\tilde{N}-m)k\Delta} \right. \\
&\quad \left. + \frac{iv}{N+1} \left(X_{t_{\tilde{N}}} \frac{1 - e^{-k(N-\tilde{N})\Delta}}{e^{k\Delta} - 1} + \sum_{j=1}^{N-\tilde{N}} Z_j \frac{e^{k\Delta} - e^{-k(N-\tilde{N}-j)\Delta}}{e^{k\Delta} - 1} \right) \right\} \\
&= \exp\left\{ iX_{t_{\tilde{N}}} e^{-k(n-\tilde{N})\Delta} \left(u + v\frac{e^{k(n-\tilde{N})\Delta} - e^{-k(N-n)\Delta}}{(e^{k\Delta} - 1)(N+1)} \right) \right. \\
&\quad \left. + i\sum_{j=1}^{n-\tilde{N}} Z_j \left(ue^{-(n-\tilde{N}-j)k\Delta} + v\frac{e^{k\Delta} - e^{-k(N-\tilde{N}-j)\Delta}}{(e^{k\Delta} - 1)(N+1)} \right) + i \sum_{j=n-\tilde{N}+1}^{N-\tilde{N}} Z_j v\frac{e^{k\Delta} - e^{-k(N-\tilde{N}-j)\Delta}}{(e^{k\Delta} - 1)(N+1)} \right\}.
\end{aligned} \tag{A.3}
$$

(i) Result (13) follows by taking the expectation of (A.3) conditional on the information at time $\tilde{t} = t_{\tilde{N}}$, and stochastic independence of $\{Z_j\}$.

(ii) Result (14) follows by additionally substituting $X_{t_{\tilde{N}}} = X_\tau = X_0 e^{-k\tau} + Z_0$ from (10) in (A.3), and taking the expectation conditional on the information at time $\tilde{t} = 0 < t_{\tilde{N}} = \tau$.

$\blacksquare$

A.2 Proof of Theorem 2

Proof. To guarantee that the Fourier transform of the lower bound (15) is well-defined, we introduce the exponential dampening factor $e^{\delta l}$ with $\delta > 0$. Then,

$$\Phi_{\tilde{t}}(u) = \int_{\mathbb{R}} e^{iul+\delta l} \left\{ \frac{e^{-r(T-\tilde{t})}}{N+1} \sum_{j=\tilde{N}+1}^{N} E_{\tilde{t}} \left[\left(e^{X_{t_j}} - \frac{(N+1)\tilde{K}}{N-\tilde{N}} \right) \mathbf{1}_{\left\{ \frac{1}{N+1} \sum_{m=\tilde{N}+1}^{N} X_{t_m} > l \right\}} \right] \right\} dl.$$

Applying Fubini's theorem yields

$$
\begin{aligned}
\Phi_{\tilde{t}}(u) &= \frac{e^{-r(T-\tilde{t})}}{N+1} \sum_{j=\tilde{N}+1}^{N} E_{\tilde{t}} \left[\left(e^{X_{t_j}} - \frac{(N+1)\tilde{K}}{N-\tilde{N}} \right) \int_{-\infty}^{\frac{1}{N+1} \sum_{m=\tilde{N}+1}^{N} X_{t_m}} e^{i(u-i\delta)l} dl \right] \\
&= \frac{e^{-r(T-\tilde{t})}}{iu+\delta} \left\{ \frac{1}{N+1} \sum_{j=\tilde{N}+1}^{N} E_{\tilde{t}} \left[e^{X_{t_j} + \frac{i(u-i\delta)}{N+1} \sum_{m=\tilde{N}+1}^{N} X_{t_m}} \right] - \tilde{K} E_{\tilde{t}} \left[e^{\frac{i(u-i\delta)}{N+1} \sum_{m=\tilde{N}+1}^{N} X_{t_m}} \right] \right\}
\end{aligned}
$$

from which (17) follows given the definition (12). Then, (16) follows by application of standard inversion formula (e.g., see Goldberg, 1961, Theorem 5C) and evaluation at $l = l^*$ given by (18).

The optimal value l^* is determined as follows. By applying the tower property of expectations in (15) we get

$$\frac{1}{N+1} \sum_{j=\tilde{N}+1}^{N} E \left[E \left(S_{t_j} - \frac{(N+1)\tilde{K}}{N-\tilde{N}} \middle| \frac{\sum_{m=\tilde{N}+1}^{N} X_{t_m}}{N+1} \right) \mathbf{1}_{\left\{ \frac{1}{N+1} \sum_{m=\tilde{N}+1}^{N} X_{t_m} > l \right\}} \right].$$

Differentiating with respect to l and interchanging with the expectation yields

$$\frac{1}{N+1} \sum_{j=\tilde{N}+1}^{N} E\left[E\left(S_{t_j} - \frac{(N+1)\tilde{K}}{N-\tilde{N}} \middle| \frac{\sum_{m=\tilde{N}+1}^{N} X_{t_m}}{N+1} \right) \frac{d}{dl} \mathbf{1}_{\left\{ \frac{1}{N+1} \sum_{m=\tilde{N}+1}^{N} X_{t_m} > l \right\}} \right]$$

$$= \frac{-h(l)}{N+1} \sum_{j=\tilde{N}+1}^{N} E\left(S_{t_j} - \frac{(N+1)\tilde{K}}{N-\tilde{N}} \middle| \frac{\sum_{m=\tilde{N}+1}^{N} X_{t_m}}{N+1} = l \right), \qquad (A.4)$$

where the last equality follows from $d\mathbf{1}_{\left\{ \sum_{m=\tilde{N}+1}^{N} X_{t_m}/(N+1) > l \right\}}/dl = -\delta\left(\sum_{m=\tilde{N}+1}^{N} X_{t_m}/(N+1) - l \right)$ with δ denoting the Dirac delta function and h the density function of $\sum_{m=\tilde{N}+1}^{N} X_{t_m}/(N+1)$. Then, (19) follows from (A.4) by setting it equal to zero. ∎

Appendix B: Computation of Price Convolutions

To compute fast the convolution (35), we employ a numerical method based on discrete Fourier transform. In what follows, we provide the details of the numerical implementation.

B.1 Implementation of Backward Induction

We compute by backward induction at each monitoring time t_{j-1}, $j = N, \ldots, 1$, the continuation value of the option which is compared with the exercise payoff of the option to determine the option value at the current time step for use one time step backward. (This method is an extended version of Lord et al., 2008 to account for the mean-reverting drift term in the log-price dynamics.) The procedure is repeated until the option value at time t_0 is obtained.

Step 0 Preliminary computations.

  a) Select equally spaced grid $\mathbf{x} := \{x_0 + m\delta\}_{m=0}^{n-1}$, for the state variable X, on which the continuation value of the option (35) is computed (see *Step 1*). The grid range is chosen based on the cumulants of $X_{t_j} - X_{t_{j-1}} e^{-k\Delta}$: $x_0 := cm_1 - \varrho\sqrt{cm_2 + \sqrt{cm_4}}$,

where ϱ is a user-defined proportionality constant and cm_j the j-cumulant (see Equations 4, 5, 7). (Cumulant cm_4 is included to ensure that the tails of the distribution are sufficiently captured.) For given grid size n, compute grid spacing $\delta := 2\varrho\sqrt{cm_2 + \sqrt{cm_4}}n^{-1}$.

b) Define grid $\mathbf{y} = \mathbf{x}$ on which the option value (37) is computed (see *Steps 2–3*).

c) Select uniform, symmetric grid $\mathbf{u} := \{(q - n/2)\delta_u\}_{q=0}^{n-1}$ of size n and spacing δ_u for use in *Step 0.d)* and *Step 1*. The range of values of the grid $\mathbf{u}$ is chosen so that the tail of the absolute value of the characteristic function of $X_{t_j} - X_{t_{j-1}}e^{-k\Delta}$, $\varphi(u;\Delta) = \exp\{iu\varepsilon(1 - e^{-k\Delta}) - \sigma^2 u^2(1 - e^{-2k\Delta})/(4k) + \xi(u)\Delta\}$, where ξ is given by (3), is sufficiently captured, i.e., $|\varphi| \leq 10^{-\varrho'}$ at the tails where $\varrho' \in \mathbb{N}$ is guided by the desired precision.

d) Let $\bar{\varphi}$ be the values of the complex conjugate of φ on the grid $\mathbf{u}$; store for use for all j in *Step 1*.

Step 1 Denote by $\tilde{\mathbf{c}}_{j-1} = \{\tilde{c}_{j-1,m}\}_{m=0}^{n-1}$ the continuation value of the option on the grid $\mathbf{x}$, $\tilde{c}(t_{j-1}; \mathbf{x})$. Compute

$$\tilde{c}_{j-1,m} := \frac{\delta_u}{2\pi}e^{i\frac{n}{2}\delta_u(\mathbf{x}-x_0)-r\Delta} \circ \sum_{q=0}^{n-1} e^{-i\frac{2\pi}{n}qm}\left(e^{-iu x_0} \circ \mathbf{G}_j \circ \bar{\varphi}\right)_q, \tag{B.1}$$

where we denote by $\mathbf{G}_j = \{G_{j,q}\}_{q=0}^{n-1}$ the values of the discrete Fourier transform of (37) on the grid $\mathbf{u}$ with

$$G_{j,q} := \delta e^{i(\mathbf{u}+\frac{n}{2}\delta_u)y_0} \circ \sum_{m=0}^{n-1} e^{i\frac{2\pi}{n}qm}\left(e^{-i\frac{n}{2}\delta_u\mathbf{y}} \circ \mathbf{g}_j \circ \mathbf{w}\right)_m \tag{B.2}$$

and $\mathbf{g}_j = \{g_{j,m}\}_{m=0}^{n-1}$ the option value on the grid $\mathbf{y}$, $g(t_j; \mathbf{y})$, initialized by (32) (see also *Step 3* for $j < N$). $\circ$ denotes the Hadamard element-wise product and $\mathbf{w} = [1/2, 1, 1, \cdots, 1, 1, 1/2]$ is the vector of trapezoid weights.

Remark 6. *The sums in (B.1) and (B.2) can be computed using the fast Fourier*

transform (FFT) which is readily available in Matlab as `fft` *and* `ifft`. *Choose grid size n to be a power of 2 for fast computation of the sums (B.1) and (B.2) using the radix-2 FFT. In addition, as required for a FFT implementation, check that the Nyquist relation $\delta_u \delta = 2\pi/n$ holds; if not, adjust the original grids accordingly. Alternatively, (B.1) and (B.2) can be re-expressed to fractional discrete Fourier transforms which discard the Nyquist restriction providing more flexibility in grid construction and can be computed using the fractional FFT, however, at a higher CPU cost (for more details about its implementation, see, e.g., Bailey and Swarztrauber, 1991).*

Step 2 Evaluate $c(t_{j-1}; \mathbf{y}) = \tilde{c}(t_{j-1}; \mathbf{y}e^{-k\Delta})$ in (36) by a cubic interpolating spline fitted to the nodes $(\mathbf{x}, \tilde{\mathbf{c}}_{j-1})$ using not-a-knot endpoint conditions (for example, use `interp1` available in Matlab).

Step 3 Compute the option values $\mathbf{g}_{j-1}$ on the grid $\mathbf{y}$ based on (37), i.e., $g(t_{j-1}; \mathbf{y}) = \max\{\psi(t_{j-1}; \mathbf{y}), c(t_{j-1}; \mathbf{y})\}$, as well as the critical value at which the exercise payoff and the continuation value coincide. Continue with *Step 1* until $j = 1$.

Remark 7. *At each monitoring time t_j, we need to identify the critical value $m_{t_j}^*$ at which the option value changes, i.e., $\psi(t_j; X_{t_j})$ and $c(t_j; X_{t_j})$ cross. This value is unknown, however it satisfies $\psi(t_j; m_{t_j}^*) - c(t_j; m_{t_j}^*) = 0$; this equation can be solved fast numerically using, for example, the Trust-Region Dogleg algorithm in Matlab with user-defined termination tolerance level and maximum number of iterations.*

References

Alesii, G., 'VaR in real options analysis', *Review of Financial Economics*, Vol. 14(3–4), 2005, pp. 189–208.

Alizadeh, A.H. and Nomikos, N.K., *Shipping Derivatives and Risk Management* (London: Palgrave McMillan, 2009).

Andersen, A., 'Valuation of shipping options', Working paper 14, Foundation for Research in Economics and Business administration (SNF), Bergen, Norway, 1992.

Andersen, L. and Andreasen, J., 'Jump-diffusion processes: Volatility smile fitting and numerical methods for option pricing', *Review of Derivatives Research*, Vol. 4(3), 2000, pp. 231–262.

Bailey, D.H. and Swarztrauber, P.N., 'The fractional Fourier transform and applications', *SIAM Review*, Vol. 33(3), 1991, pp. 389–404.

Bakshi, G., Cao, C. and Chen, Z., 'Empirical performance of alternative option pricing models', *The Journal of Finance*, Vol. 52(5), 1997, pp. 2003–2049.

Bates, D.S., 'Jumps and stochastic volatility: exchange rate processes implicit in deutsche mark options', *The Review of Financial Studies*, Vol. 9(1), 1996, pp. 69–107.

Bjerksund, P. and Ekern, S., 'Contingent claims evaluation of mean-reverting cash flows in shipping', in L. Trigeorgis, ed., *Real Options in Capital Investment: Models, Strategies, and Applications* (Westport: Praeger, 1995), pp. 207–219.

Brennan, M. and Schwartz, E.S., 'Evaluating natural resource investments'. *The Journal of Business*, Vol. 58(2), 1985, pp. 135–157.

Cont, R. and Tankov, P., *Financial Modelling With Jump Processes* (Boca Raton: Chapman & Hall/CRC, 2004).

Cortazar, G., Schwartz, E.S. and Salinas, M., 'Evaluating environmental investments: A real options approach', *Management Science*, Vol. 44(8), 1998, pp. 1059–1070.

Curran, M., 'Valuing Asian and portfolio options by conditioning on the geometric mean price', *Management Science*, Vol. 40(12), 1994, pp. 1705–1711.

Dixit, A.K., 'Entry and exit decisions under uncertainty', *Journal of Political Economy*, Vol. 97(3), 1989, pp. 620–638.

Dixit, A.K. and Pindyck, R.S., *Investment Under Uncertainty* (Princeton, New Jersey: Princeton University Press, 1994).

Fusai, G. and Kyriakou, I., 'General optimized lower and upper bounds for discrete and continuous arithmetic Asian options', *Mathematics of Operations Research*, Vol. 41(2), 2016, pp. 531–559.

Geman, H., *Commodities and Commodity Derivatives: Modeling and Pricing for Agriculturals, Metals and Energy* (Chichester: John Wiley & Sons, Ltd, 2005).

Goldberg, R.R., *Fourier Transforms* (Cambridge: Cambridge University Press, 1961).

Greenwood, R. and Hanson, S.G., 'Waves in ship prices and investment', *The Quarterly Journal of Economics*, Vol. 130(1), 2015, pp. 55–109.

Grenadier, S.R., 'The strategic exercise of options: Development cascades and overbuilding in real estate markets', *The Journal of Finance*, Vol. 51(5), 1996, pp. 1653–1679.

Hilliard, J.E. and Reis, J.A., 'Jump processes in commodity futures prices and options pricing', *American Journal of Agricultural Economics*, Vol. 81(2), 1999, pp. 273–286.

Jørgensen, P.L. and De Giovanni, D., 'Time charters with purchase options in shipping: Valuation and risk management', *Applied Mathematical Finance*, Vol. 17(5), 2010, pp. 399–430.

Kalouptsidi, M., 'Time to build and fluctuations in bulk shipping', *American Economic Review*, Vol. 104(2), 2014, pp. 564–608.

Kandel, E. and Pearson, N.D., 'Option value, uncertainty, and the investment decision', *Journal of Financial and Quantitative Analysis*, Vol. 37(3), 2002, pp. 341–374.

Kellogg, R., 'The effect of uncertainty on investment: Evidence from Texas oil drilling', *American Economic Review*, Vol. 104(6), 2014, pp. 1698–1734.

Kilian, L., 'Not all oil price shocks are alike: Disentangling demand and supply shocks in the crude oil market', *American Economic Review*, Vol. 99(3), 2009, pp. 1053–1069.

Koekebakker, S., Adland, R. and Sødal, S., 'Pricing freight rate options', *Transportation Research Part E: Logistics and Transportation Review*, Vol. 43(5), 2007, pp. 535–548.

Kyriakou, I., Nomikos, N.K., Papapostolou, N.C. and Pouliasis, P.K., 'Affine-structure models and the pricing of energy commodity derivatives', *European Financial Management* Vol. 22(5), 2016, pp. 853–881.

Levy, E., 'Asian options', in L. Clewlow, C. Strickland, eds., *Exotic Options: The State of the Art* (Washington DC: International Thomson Business Press), pp. 65–91.

Longstaff, F.A. and Schwartz, E.S., 'Valuing American options by simulation: A simple least-squares approach', *The Review of Financial Studies*, Vol. 14(1), 2001, pp. 113–147.

Lord, R., Fang, F., Bervoets, F. and Oosterlee, C.W., 'A fast and accurate FFT-based method for pricing early-exercise options under Lévy processes', *SIAM Journal on Scientific Computing*, Vol. 30(4), 2008, pp. 1678–1705.

Majd, S. and Pindyck, R.S., 'Time to build, option value, and investment decisions', *Journal of Financial Economics*, Vol. 18(1), 1987, pp. 7–27.

McDonald, R. and Siegel, D., 'The value of waiting to invest', *The Quarterly Journal of Economics*, Vol. 101(4), 1986, pp. 707–727.

Moel, A. and Tufano, P., 'When are real options exercised? An empirical study of mine closings', *The Review of Financial Studies*, Vol. 15(1), 2002, pp. 35–64.

Nomikos, N.K., Kyriakou, I., Papapostolou, N.C. and Pouliasis, P.K., 'Freight options: Price modelling and empirical analysis', *Transportation Research Part E: Logistics and Transportation Review*, Vol. 51, 2013, pp. 82–94.

Papapostolou, N.C., Nomikos, N.K., Pouliasis, P.K. and Kyriakou, I., 'Investor sentiment for real assets: The case of dry bulk shipping market', *Review of Finance*, Vol. 18(4), 2014, pp. 1507–1539.

Pindyck, R.S., 'Irreversibility, uncertainty, and investment', *Journal of Economic Literature*, Vol. 29(3), 1991, pp. 1110–1148.

Politis, D.N. and Romano, J.P., 'The stationary bootstrap', *Journal of the American Statistical Association*, Vol. 89(428), 1994, pp. 1303–1313.

Rogers, L.C.G. and Shi, Z., 'The value of an Asian option', *Journal of Applied Probability*, Vol. 32(4), 1995, pp. 1077–1088.

Samuelson, P.A., 'Proof that properly anticipated prices fluctuate randomly', *Industrial Management Review*, Vol. 6(2), 1965, pp. 41–49.

Schwartz, E. and Smith, J.E., 'Short-term variations and long-term dynamics in commodity prices', *Management Science*, Vol. 46(7), 2000, pp. 893–911.

Schwartz, E.S. and Zozaya-Gorostiza, C., 'Investment under uncertainty in information technology: Acquisition and development projects', *Management Science*, Vol. 49(1), 2003, pp. 57–70.

Sødal, S., Koekebakker, S. and Aadland, R., 'Market switching in shipping – A real option model applied to the valuation of combination carriers', *Review of Financial Economics*, Vol. 17(3), 2008, pp. 183–203.

Sødal, S., Koekebakker, S. and Adland, R., 'Value based trading of real assets in shipping under stochastic freight rates', *Applied Economics*, Vol. 41(22), 2009, pp. 2793–2807.

Sullivan, R., Timmermann, A. and White, H., 'Data-snooping, technical trading rule performance, and the bootstrap', *The Journal of Finance*, Vol. 54(5), 1999, pp. 1647–1691.

United Nations Conference on Trade and Development (UNCTAD), *Review of Maritime Transport* (New York: United Nations Publications, 2015).

Triantis, A.J. and Hodder, J.E., 'Valuing flexibility as a complex option', *The Journal of Finance*, Vol. 45(2), 1990, pp. 549–565.

Turnbull, S.M. and Wakeman, L.M., 'A quick algorithm for pricing European average options', *Journal of Financial and Quantitative Analysis*, Vol. 26(3), 1991, pp. 377–389.

Tvedt, J., 'Valuation of VLCCs under income uncertainty', *Maritime Policy & Management*, Vol. 24(2), 1997, pp. 159–174.

Zhang, P.G., 'An introduction to exotic options', *European Financial Management*, Vol. 1(1), 1995, pp. 87–95.

Table 1: Model calibration results for the Baltic Capesize Index

The table is divided in two panels. Panel A of the table provides the implied risk neutral BCI model parameters. Estimation has been performed on a weekly basis in the period 04 January 2008 to 27 June 2014 over all options ("All options") and maturity-partitioned datasets (+Q, +1CAL, +2CAL). The reports in Panel A are the averages (across weeks) of the annual parameter estimates of the fitted MRJ model along with their standard errors in ($\cdot$). Panel B reports the averages (across weeks) of the option pricing error statistics MAPE (21) and RMSPE (22) under the MRJ model. For out-of-sample pricing errors, on each Friday, we use in-sample model estimates to price the same options one week later using the relevant spot prices, time to maturities and interest rates. We assess the MRJ model fit by considering the MAPE and RMSPE statistics and testing the null hypothesis that MRJ does not perform better than a benchmark by employing the stationary bootstrap of Politis and Romano (1994) with 10,000 bootstrap simulations. As benchmarks, we consider the MR and LogN models which we calibrate using the same dataset. Superscripts a and b indicate that MRJ yields significantly lower pricing errors than LogN and MR, respectively, at the 1% significance level.

Panel A. Model parameters						
	k	ε	σ	λ	μ_J	σ_J
Estimate	3.310	2.486	0.688	6.786	-0.272	0.736
Standard error	(0.133)	(0.043)	(0.042)	(0.198)	(0.005)	(0.007)

Panel B. Pricing errors				
	All options	+Q	+1CAL	+2CAL
In-sample pricing errors				
MAPE	$0.1191^{a,b}$	$0.1773^{a,b}$	$0.1073^{a,b}$	$0.0778^{a,b}$
RMSPE	$0.1699^{a,b}$	$0.2212^{a,b}$	$0.1376^{a,b}$	$0.0920^{a,b}$
Out-of-sample pricing errors				
MAPE	$0.1612^{a,b}$	$0.2352^{a,b}$	$0.1463^{a,b}$	$0.1087^{a,b}$
RMSPE	$0.2335^{a,b}$	$0.2857^{a,b}$	$0.1830^{a,b}$	$0.1421^{a,b}$

Table 2: Regression analysis of pricing errors

The table reports the coefficients of the regression equation (23) for the MRJ model option pricing errors computed using the parameter estimates in Table 1. Standard errors $(\cdot)$ are corrected for serial correlation and heteroscedasticity. F-statistics are used to test the joint null hypothesis H_0: $\beta_1 = \beta_2 = \beta_3 = \beta_4 = 0$. As benchmarks, we consider the MR and LogN models which we calibrate using the same dataset; adj. R^2 and F-statistics for the MR and LogN models are also reported. Superscripts a, b and c indicate significance of the coefficients at the 1%, 5% and 10% levels, respectively.

		MRJ model				MR model	LogN model
β_0	β_1	β_2	β_3	β_4	adj. R^2	adj. R^2	adj. R^2
					F-stat	F-stat	F-stat
In-sample pricing errors							
-0.0852^a	0.1270^a	-0.0488^a	0.0011	0.0104^b	1.73%	5.24%	10.19%
(0.022)	(0.026)	(0.008)	(0.016)	(0.004)	53.12^a	163.7^a	336.1^a
Out-of-sample pricing errors							
-0.0660^c	0.0845^b	-0.0430^a	0.0059	0.0268^a	1.31%	5.39%	7.97%
(0.038)	(0.040)	(0.013)	(0.031)	(0.008)	40.19^a	168.1^a	255.6^a

Table 3: Capesize vessel valuation results

The table reports values (in million USD) of vessels of different ages based on the parameter estimates in Table 1. The table also presents sensitivities of the vessel price V with respect to the scrap price $\bar{V}$, interest rate r, and model parameters $\exp(\varepsilon)$, k, σ and λ. For the newbuilding (NB) vessel with $l = 2$, we also report the sensitivity of V with respect to the construction lag l. For exposition purposes, all sensitivities are expressed in monetary terms (million USD) and have been rescaled in order to correspond to changes of 1 million USD in $\bar{V}$, 1 basis point in r, 100 USD in $\exp(\varepsilon)$, 0.5 in k, 1% in σ, 0.5 in λ and 0.25 years in l. All calculations are based on an initial spot rate of 34,700 USD (spot BCI 4TC), a scrap price of 9.5 million USD (capesize) and an interest rate of 3.9% per annum.

Vessel age	Vessel price (million USD)	Vessel price sensitivities (million USD)						
	V	$\partial V/\partial \bar{V}$	$\partial V/\partial r$	$\partial V/\partial \exp(\varepsilon)$	$\partial V/\partial k$	$\partial V/\partial \sigma$	$\partial V/\partial \lambda$	$\partial V/\partial l$
Newbuilding vessels								
NB ($l = 2$)	60.165	0.348	-0.077	0.473	-0.309	0.059	-0.480	-0.725
NB ($l = 0$)	68.038	0.376	-0.072	0.518	-0.609	0.066	-0.441	–
Secondhand vessels								
5Y	61.541	0.457	-0.055	0.457	-0.569	0.058	-0.327	–
10Y	53.209	0.556	-0.038	0.380	-0.519	0.048	-0.214	–
15Y	42.528	0.676	-0.022	0.282	-0.456	0.036	-0.111	–
20Y	28.838	0.822	-0.009	0.156	-0.374	0.020	-0.033	–

Table 4: Optimal exercise time of option to invest

The table reports the summary statistics (mean, standard error and interquartile range) of the optimal exercise time t_{opt} (in years) of the option to invest in a vessel of a given age, as well as the simulated distribution of the optimal exercise time based on 10,000 Monte Carlo simulations. We consider vessels of different ages and use the parameter estimates in Table 1.

	Newbuilding vessels		Secondhand vessels			
	$l = 2$	$l = 0$	5Y	10Y	15Y	20Y
Optimal exercise time summary statistics						
Mean	0.147	2.084	2.176	2.157	2.400	2.440
Standard error	0.002	0.095	0.097	0.100	0.103	0.102
Interquartile range	0.00	4.00	4.17	4.17	5.00	4.85
Optimal exercise time distribution						
$t_{opt} \leq 1$	100.0%	62.4%	60.9%	63.1%	58.9%	57.0%
$1 < t_{opt} \leq 4$	0.0%	12.7%	13.5%	11.5%	12.2%	14.4%
$4 < t_{opt} \leq 7$	0.0%	12.8%	12.8%	11.9%	13.4%	14.5%
$t_{opt} > 7$	0.0%	12.1%	12.8%	13.5%	15.5%	14.1%

Fig. 1: Drybulk supply and demand

The figure presents the year-on-year % change in world fleet development and seaborne trade. Source: Clarkson Shipping Intelligence Network (as of October 2015).
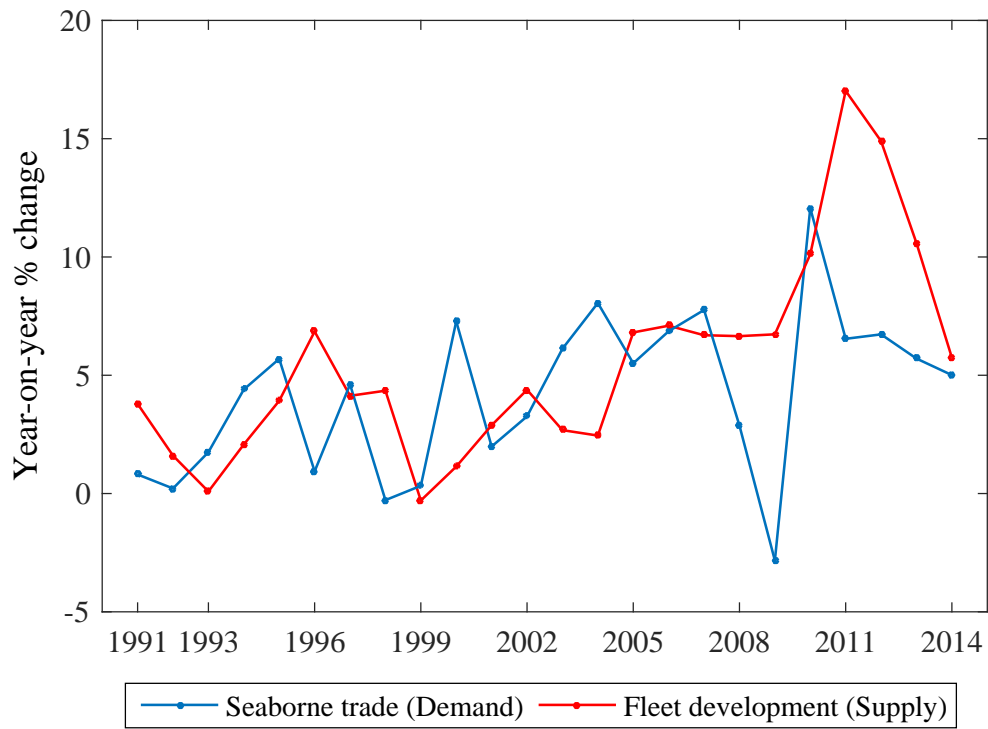
Fig. 2: Estimated volatility, skewness and excess kurtosis of BCI log-changes

The figure presents the weekly evolutions of the implied volatility (Eq. 5), skewness and excess kurtosis (Eq. 8) of the 1-week, 1-month and 1-year log-changes in the BCI computed using the parameter estimates in Table 1.
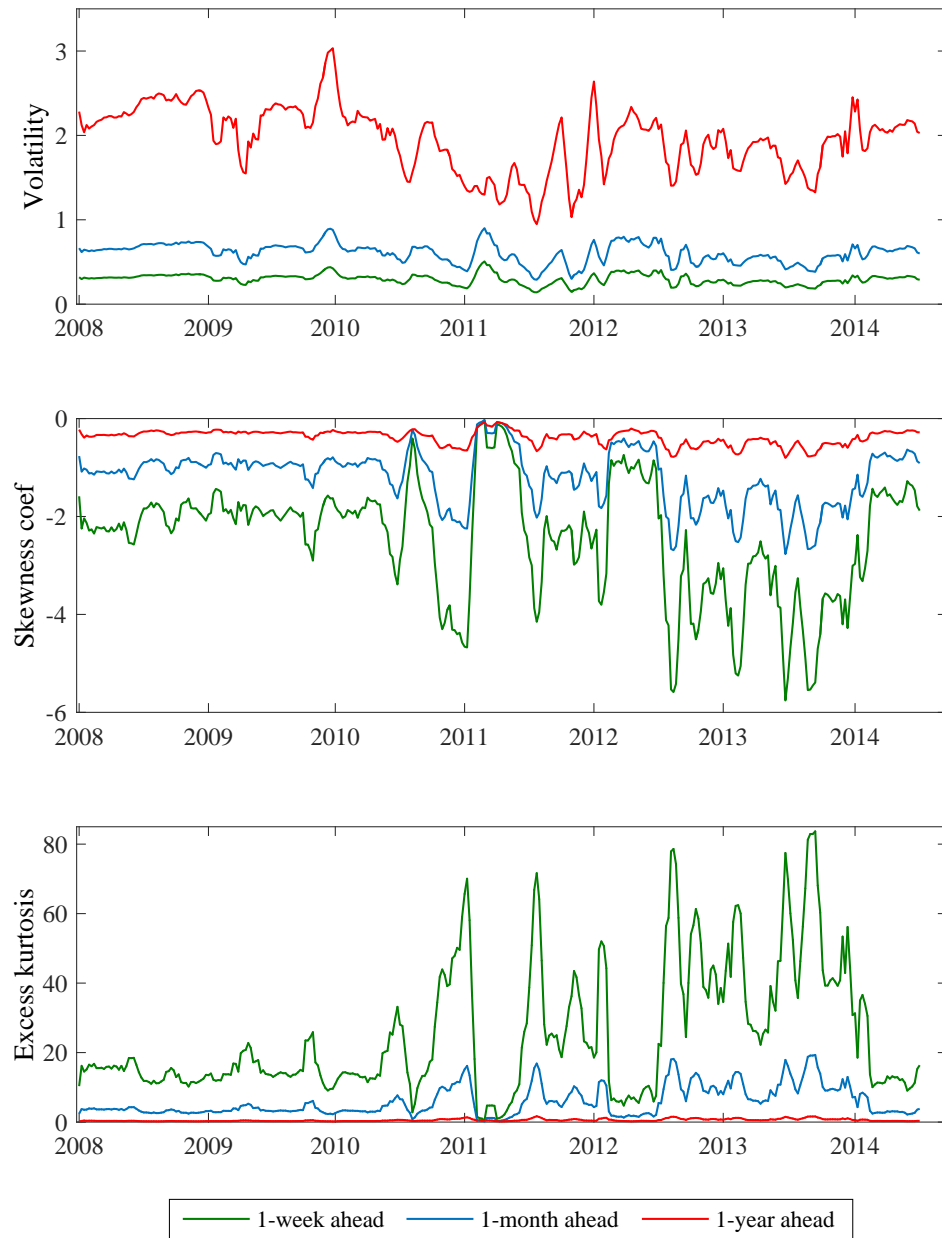
Fig. 3: Capesize vessel valuation results

The top-left sub-figure presents the model capesize vessel values (in million USD) computed using formula (24) for different vessel ages based on the parameter estimates in Table 1, as well as the historical mean capesize vessel values along with the 5th and 95th percentiles. Calculations are based on an initial spot rate of 34,700 USD, a scrap price of 9.5 million USD and an interest rate of 3.9% per annum (average values across our sample period). The remaining sub-figures depict the annual average prices of vessels of different ages across different years and the corresponding model prices computed using the average parameters, spot rates, scrap prices and interest rates for the year of interest.
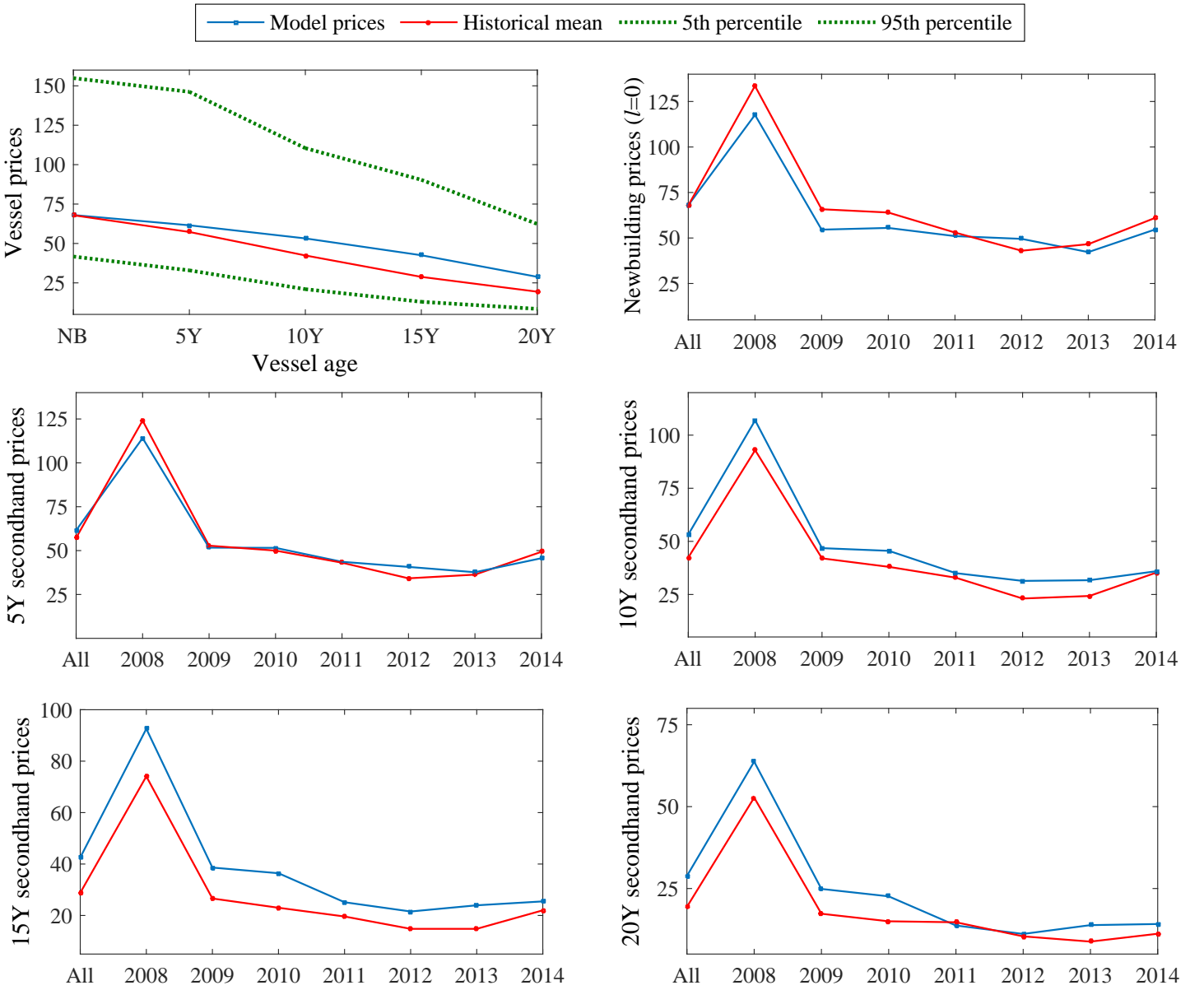
Fig. 4: Vessel price patterns for varying parameter values

The figure presents vessel price patterns (in million USD) for varying initial spot freight rate S_0 (in thousand USD), for given deviations from the estimated (see Table 1 and indicated parameter values by an asterisk in this figure) long-run freight level $\exp(\varepsilon)$ (in thousand USD), half-life $\ln 2^{1/k}$ (in months), jump arrival rate λ and diffusion coefficient σ. For illustrative purposes, we present the case of the newbuilding vessel without construction lag.
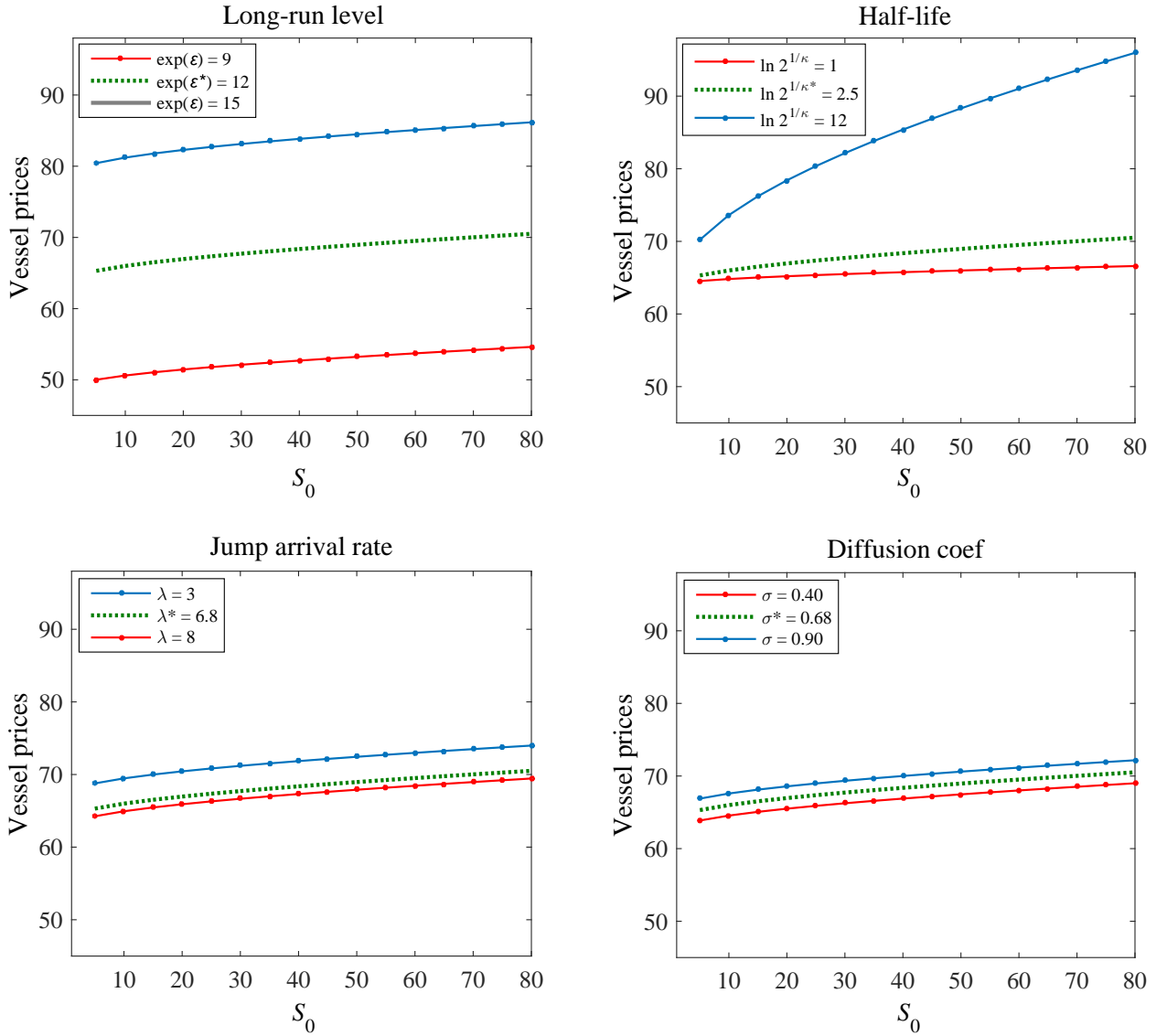
Fig. 5: Net present value profiles of investments in vessels

The figure presents, for different vessel ages, real option NPVs (dark surfaces) versus conventional NPVs (white surfaces) for varying long-run freight level $\exp(\varepsilon)$ (in thousand USD) and diffusion coefficient σ. The zero plane (grey surface) is also plotted for reference. All NPVs are in million USD.
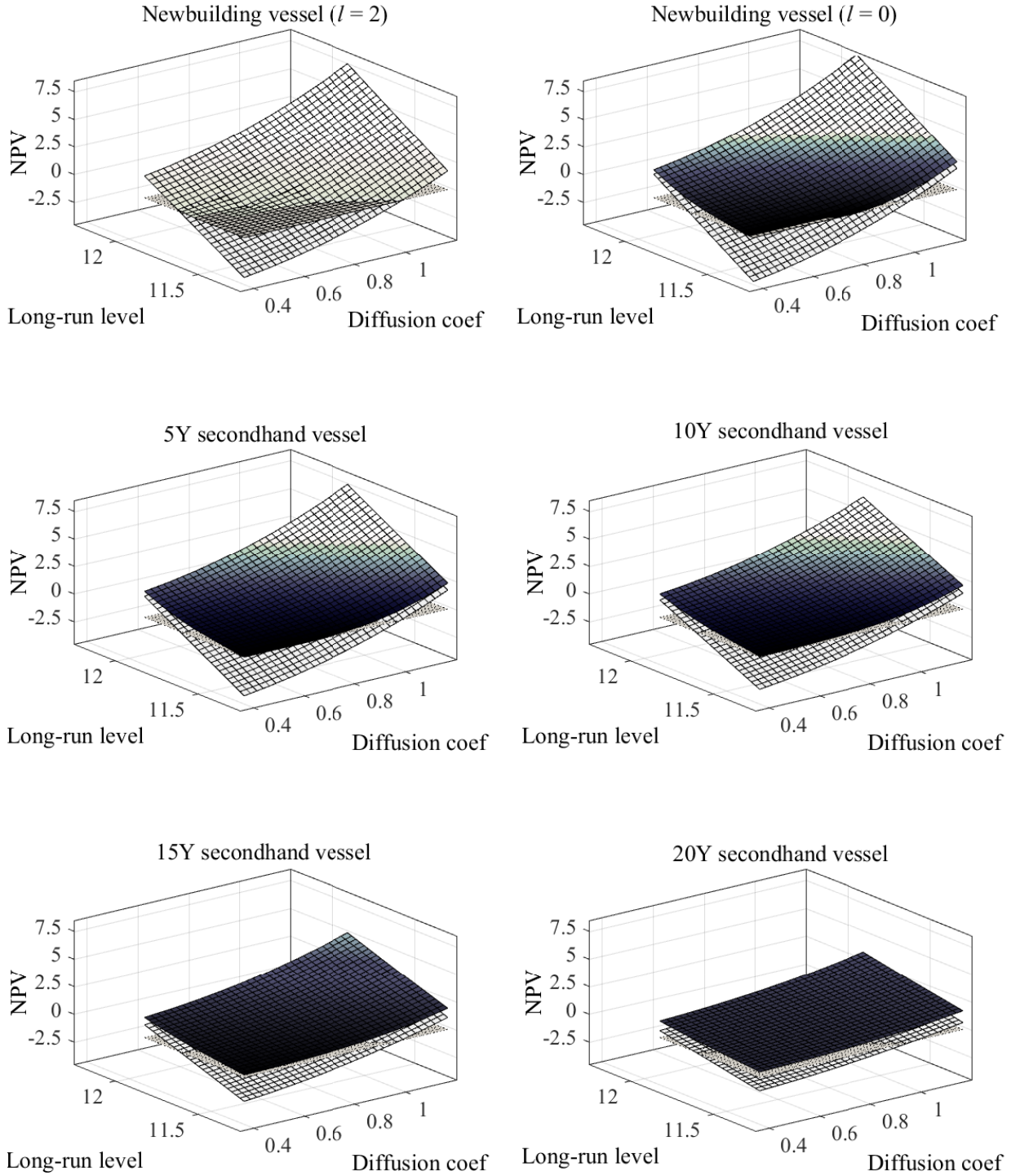
Fig. 6: Distribution of optimal exercise time of option to invest

The figure presents simulated probability density estimates of the mean optimal exercise time (in years) of the option to invest in a vessel of a given age. Each density is based on computed mean optimal exercise times for 825 different combinations of the long-run freight level $\exp(\varepsilon)$ and diffusion coefficient σ.